

HIGH ENERGY HEAVY ION INDUCED
ENHANCED ADHESION

Thesis by

Marcus H. Mendenhall

In Partial Fulfillment of the Requirements
for the Degree of
Doctor of Philosophy

California Institute of Technology
Pasadena, California

1983

(Submitted April 26, 1983)

Acknowledgements

First, I would like to thank my wife, Cheryl, for all of the moral support she provided while I was working on this project, and for her deep insights into the reason adhesion really works (See Fig. 22.) Also, Dr. T. Tombrello, my advisor, was not only a very good advisor from a scientific point of view, he was also a very good friend and gave a great deal of advice about things not related to the project that is greatly appreciated.

Many people at Caltech provided a lot of help: Joe Griffith started this whole project while he was here; Yuanxun Qiu provided invaluable insights and help; Dr. Ricardo Schwarz provided lots of ideas, and lots of enthusiasm; Dr. R. Kavanagh provided lots of help running the EN tandem when it was misbehaving; Dr. B. X. Liu and Dr. Bruce Paine provided the multilayer silver on silicon target; Dr. T. Vreeland allowed the use of his facilities by Brad Werner for analyzing our samples; Brad Werner did a great deal of work looking for mixed layers; Wil Shick, Bob Stevens and Don Woshnak provided excellent assistance and advice in the shop; Marty Watson, Kim Stapp, Jan Rasmussen and Michelle Vine provided friendly and effective secretarial assistance. Thanks are also due Tom Skelton and John Osborne, who prevented me from going stark raving sane; and to many other people around campus who provided help in many facets of this project. Elsewhere, Dr. R. Stokstad and the staff of the LBL 88" cyclotron lab were invaluable in providing beam time and help while running there.

Thanks are due the National Science Foundation, which contributed both research funds to the project and support to me in the form of an NSF graduate fellowship. Thanks also go to IBM, which supplied an IBM graduate fellowship to support my final year of graduate study.

Thanks are also due to my parents, who gave me the great opportunities in life to be the places I have been that eventually brought me here.

Finally, my greatest thanks to the Lord God, who made all of this possible and to whom this thesis is dedicated.

ABSTRACT

The work described in this thesis represents an attempt to summarize to date the information collected on the process of high energy heavy ion induced enhanced adhesion. Briefly, the process involves the irradiation of materials covered by thin ($\lesssim 3\mu\text{m}$) films with high energy ($E > 200 \text{ keV / nucleon}$) heavy ion beams (such as Fluorine or Chlorine). Enhanced adhesion has been observed on all material combinations tested, including metal on metal, metal on semiconductor, metal on dielectric and dielectric on dielectric systems. In some cases, the enhancement can be quite large, so that a film that could be wiped off a substrate quite easily before irradiation can withstand determined scrubbing afterwards.

Very little is understood yet about this adhesion mechanism, so what is presented are primarily observations about systems studied, and descriptions of the actual preparation and irradiation of samples used. Some discussion is presented about mechanisms that have been considered but rejected.

Table of Contents

| | | |
|-------------------|--|-----|
| Acknowledgements | | ii |
| Abstract | | iii |
| Table of Contents | | iv |
| §1 | Background and Overview | 1 |
| 1.1 | Previous Adhesion Work | 1 |
| 1.2 | Origin of High Energy Heavy Ion Induced Adhesion | 2 |
| §2 | The Care and Feeding of Samples | 5 |
| 2.1 | Sample Preparation | 5 |
| 2.1.1 | Dielectrics and Metals | 5 |
| 2.1.2 | Silicon | 5 |
| 2.1.3 | Indium Phosphide and Gallium Arsenide | 6 |
| 2.1.4 | I-carbon films | 6 |
| 2.2 | Sample Irradiation | 6 |
| §3 | Adhesion Measurement | 8 |
| 3.1 | The "Scotch Tape" Test | 8 |
| 3.2 | The Loudspeaker Tester | 9 |
| §4 | Discussion of Specific Experiments | 12 |
| 4.1 | Rutherford Backscattering Measurement of Mixing Depth | 12 |
| 4.1.1 | Early Attempts using Low Resolution | 12 |
| 4.1.2 | High Resolution Measurement of Mixing of Ag on Si | 13 |
| 4.2 | Electron Diffraction and TEM Analysis | 15 |
| 4.3 | Dependence of Threshold Adhesion on dE/dx | 15 |
| §5 | Possible Mechanisms, and Why They Are Wrong | 17 |
| 5.1 | Nuclear Collision Driven Mixing | 17 |
| 5.2 | Thermalized Ion Explosion Driven Mixing | 18 |
| §6 | Random Observations about Samples | 20 |
| 6.1 | Behavior of Silicon with Different Cleaning Procedures | 20 |
| 6.2 | Enhanced Adhesion and Wettability | 21 |
| 6.3 | Electrical Contact Properties of Metals on Semiconductors | 22 |
| 6.4 | Damage to Compound Semiconductors | 23 |
| §7 | Conclusions | 23 |
| Table 1 | | 26 |
| Table 2 | | 29 |
| Figures | | 30 |
| Bibliography | | 64 |

1. Background and Overview

1.1. Previous Adhesion Work

The problem of bonding materials together is an old and important one. Before thin film techniques became important, most bonding was done by using various macroscopic mechanical means such as glues and welding. However, with thin films, such techniques are not very practical. The first problem is that the films often have little strength, so that bonding a film to a backing at one point does not assure that it will not peel somewhere else. This precludes the use of most forms of welding to attach films. Also, many systems where thin films are used are sensitive to heat, so that many high temperature processes like welding are excluded for that reason. Chemical bonding is often impossible, since this requires a layer of some extraneous material to lie between the film and its substrate. Since many applications of thin films depend on the direct contact of the film to the substrate, the intervening layer is unacceptable. In some cases, thin films are bonded to backings by introducing another thin film in between that sticks to both the film and the substrate, hence bonding the two together. This is often a compromise, though, trading off the desired properties of the direct bond for the mechanical strength obtained this way.

Another method used to bond thin films is low energy ion beam mixing. In this process, ions with sufficiently low energy that the nuclear component of the stopping power predominates ($E < 0.1$ MeV/amu) are used. These ions directly strike the lattice ions of the material, causing ions to be displaced over fairly long distances, mixing the atoms across the interface. (See Fig. 1) This process is used extensively on systems where the two materials involved form stable chemical compounds, so that by mixing up the interface a strong bond is formed by the compound. This technique has a number of drawbacks that limit its usefulness in many systems. First, it implants a large number of ions ($> 1 \times 10^{16} / \text{cm}^2$) within about $1 \mu\text{m}$ of the surface. Since many systems have active regions of the order of this thickness, the ions may end up inside a part of the material where they will degrade or destroy the performance of the device. Second, low energy ions beams mix a layer that can be of the order of 50 nm thick. In many thin film applications, this is

a significant fraction of the total thickness of the film and may therefore substantially affect the properties of the film. The third drawback to low energy ion beam mixing for adhesion enhancement is that low energy ion beams typically have large sputtering yields on most materials, so that in the process of bonding films, much of the film may be sputtered away. Because of the simplicity of this method, which requires a very small accelerator and simple setup, it has gained wide acceptance among thin film workers.

1.2. Origin of High Energy Heavy Ion Induced Adhesion

The idea of using high energy ion beams to induce adhesion was developed by Griffith and Qiu in 1981 (Gr82). It was thought that since high energy heavy ions make damage tracks in dielectric materials (Fl75), it might be possible to use the damage to disturb the interface between a dielectric and some other material. By disturbing the interface, some mixing might be induced which would bond the materials together. This was thought to have particularly interesting applications in the case of a metal on a dielectric substrate. Since electrical conductors show very little damage from high energy heavy ions, and have a very low sputtering yield, it should be possible to bond such a material to its substrate without affecting the properties of the film significantly. (See Fig. 2) This could have many useful applications in optical systems and mechanical systems where the properties of the film are critical. Because high energy heavy ions produce a plasma along their path that has a thermal energy distribution (Se82), there are very few ions that obtain very high energy, so one would expect the mixing layer to be very thin in systems like this (as opposed to low energy ions, in which the energy distribution falls off as a power law at high energy, so there are some quite energetic ions produced, hence deep mixing is generated). (See Fig. 3) Thus, with possibly very minimal disturbance to the interface, the materials might be bonded.

This technique was tested on a few systems of interest, and it was found to work quite well. The substrates first tried were teflon, fused quartz and ferrite. The film applied in all cases was gold. With teflon, a dose of $1 \times 10^{14} / \text{cm}^2$ of 1 MeV protons was found to be sufficient to cause strong adhesion. On quartz and ferrite, heavier ions (10 MeV Fluorine or

20 MeV Chlorine) and higher doses ($1 \times 10^{15} / \text{cm}^2$) were required. At this point it was assumed that the track formation model for adhesion was approximately correct.

Sometime later, people who were working with semiconductors asked if it was possible by this technique to bond films to semiconductors. The answer was that it shouldn't be, but it was worth a try anyway. Since semiconductors were expected to show, at best, a very weak effect, very large doses ($1 \times 10^{16} / \text{cm}^2$) of 20 MeV Cl were tried at first on a gold on silicon film. We soon found out that rather than requiring higher doses than dielectrics, semiconductors required comparable or even lower doses to obtain very good adhesion. This led us in the obvious direction of trying metal on metal systems, where there was no doubt that the dielectric track formation mechanism would not occur. When it was found that metal on metal systems require some of the lowest doses for adhesion of any systems we had tried, we decided that the effect must be quite independent of track formation in dielectrics. (See Table 1 for a complete list of systems tested and Fig. 4 for pictures of typical samples.)

After we became fairly confident that the mechanism was not the simple track formation mechanism that was originally proposed, we were left with the problem of trying to see if there was any other simple mechanism to be found. The first thing we did was to look for a mixed layer at the interface. Rutherford backscattering was tried first, since it was the easiest technique for looking for a mixed layer, if the layer were not too thin. By using multilayer targets, we determined that the mixing was on a depth scale of less than 1 nm, but this was only an upper limit since that was approximately our resolution. We then proceeded to transmission electron microscopy (TEM) and electron diffraction to see if any new crystal formation could be detected. Although spotty regions of new crystal were seen, nothing was seen often enough to believe that it could be the cause of adhesion.

The lack of success in seeing any significant mixing prompted us to change our strategy in the search for a mechanism. We started developing adhesion measurement techniques so that we could determine the actual strength of the bond developed by this technique, and how that strength depends on the beam parameters. Also, we mapped out how the beam dose at fixed adhesion strength depends on the energy loss of the

beam in the materials. This was done with the hope that the result would allow some simple model to be developed for the energy transfer process occurring. The one important piece of information that came out of this work was that the adhesion process depends on dE/dx differently in metal-dielectric systems than in metal-metal systems, so that instead of a single mechanism, there are probably at least two.

2. The Care and Feeding of Samples

(See Table 1 for a list of samples tested.)

2.1. Sample Preparation

2.1.1. Dielectrics and Metals

Dielectric samples such as fused silica, teflon, alumina and ferrite and metals such as tungsten and tantalum were cleaned before film deposition as follows: First, the samples were washed in hot water and Alconox detergent in an ultrasonic bath. Then, after rinsing in deionized water, they were dipped for about 20 minutes in a boiling concentrated $\text{HNO}_3\text{:H}_2\text{O}$ 1:1 solution. They were then rinsed in deionized water and dried in reagent grade methanol. Then, they were loaded into a bell jar and the film was thermally deposited when the pressure was below 2×10^{-6} Torr.

2.1.2. Silicon

Silicon samples were precleaned in hot water and Alconox. They were then dipped in concentrated $\text{HF:H}_2\text{O}$ 1:1 for about 20 minutes. In some cases they were then rinsed in deionized water and loaded into the bell jar. In other cases they were first rinsed in methanol before loading into the jar, and a few times they were rinsed in methanol with about 5% Br added (as recommended by P. C. Chen in his thesis, Ch81). The various preparation techniques seemed to make no real difference in the behavior of the films. The metal films were deposited when the pressure was below 2×10^{-6} Torr. With gold on silicon films, the adhesion before irradiation was occasionally sufficiently good that the films already passed the Scotch Tape test (see §3.1). With silver on silicon, the adhesion was usually very weak before irradiation.

One silicon sample that was used was prepared at China Lake Naval Weapons Center under ultra high vacuum conditions. The substrate was a fused silica disk, which was sputter cleaned and 100 nm of silicon was deposited on it. Then, without breaking vacuum, a silver film was deposited on this sample, so that there should be no intervening layer of any adsorbed material between the silver and the silicon. This sample showed fairly high adhesion before irradiation, but as it sat exposed to air, the film slowly peeled around the edges. However, the irradiated areas did

not peel, so by waiting for air to affect the film we could still test it for improved adhesion.

2.1.3. Indium Phosphide and Gallium Arsenide

These samples were washed in Alconox and hot water, and then rinsed in methanol. The evaporation was done as before. However, because these materials are extremely fragile, they were usually taped onto glass microscope slides to provide some support and reduce breakage. Because tape does not fare very well in vacuum, the pressure at which many of these samples were prepared was about 5×10^{-6} Torr. However, experience shows that adhesion of films deposited at pressures as high as 1×10^{-5} Torr is no different than the adhesion of films produced at much lower pressures.

2.1.4. I-carbon Films

First, an explanation of what an I-carbon film is in order. These are very hard films of carbon, deposited from a plasma, that are electrically insulating and nearly transparent, even in layers up to $1 \mu\text{m}$ thick. It is thought that they have a diamond-like structure. They adhere fairly weakly to most substrates, and are quite brittle. The films we received came from China Lake Naval Weapons Center and were deposited on silicon and calcium fluoride substrates. The films on CaF_2 were much more fragile than the ones on Si, and tended to disintegrate spontaneously.

These films could not be cleaned in any kind of hot acid bath without having them peel immediately, so that the only cleaning possible was a methanol rinse. Thus, we cannot be sure that these films were as clean as other films which we used.

2.2. Sample Irradiation

The irradiations for this project were done primarily on the Caltech CIT-ONR EN tandem Van de Graaff accelerator. Samples irradiated with krypton and argon and oxygen were processed at the LBL 88 inch cyclotron.

When irradiations were done with the EN tandem, samples were mounted on a hexagonal aluminum target holder in a scattering chamber so that the target could be rotated about the vertical axis and translated

vertically. The rotation was used to control the horizontal position of the beam on the surface of the target. The maximum deviation of target from the beam normal was 20° so that the biggest error in the fluence resulting from the angle would be about 6%, because $\cos(20^\circ) \cong .94$. The faces of the hexagon were 2.54 cm wide so fairly large samples could be easily accommodated.

The target holder was operated at a bias of +600 volts to assure good secondary electron suppression. Also, it was surrounded by a screen cage biased to -2000 volts to suppress secondary electron spray coming down the beam tube, and to increase the effective target bias. The voltages are sufficiently high that the current integration should be accurate to a few percent. There was no significant change in indicated current on the target with the cage bias anywhere between -1000 V and -5000 V. When running with much over -2000 V on the cage, though, sparking from the cage became a problem, so the voltage was not normally run above this value.

Samples for which beam dose and uniformity were critical were irradiated through a 2.4 mm quartz collimator with the beam defocused to obtain a very uniform intensity over the hole. The collimator was outside of the electron suppression cage, so electron spray from it should not have affected the current integration. Also, the geometry of the collimator holder made it a fairly effective Faraday cup, so it was possible to read beam current on it as well as on the target. By focusing the beam entirely through the collimator and then steering it from the target onto the collimator, the current integration on the collimator was verified to be good to better than 10%. Under normal operating conditions, with the beam defocused on the collimator, between 10% and 30% of the total beam current was going through the collimator onto the target. The uniformity of intensity could be verified by steering the spot around on the collimator and noting the change in the current passing through the hole. By this technique, we are fairly confident that the dose can be made uniform to better than 10%. Samples where uniformity and accuracy of dose measurement were not critical were irradiated with the beam collimated by a set of movable slits upstream of the target chamber. (See Fig. 5 for a sketch of the target arrangement.)

At the LBL 88 inch cyclotron the apparatus was similar, but had some differences. The target was mounted on a holder with only vertical motion, and the collimator was mounted so that it had horizontal motion. Thus, by moving the collimator and steering the beam through the hole, spots could be produced in horizontal rows on the target. This had the advantage that the target was always at 90° to the beam. (See Fig. 6 for a sketch of the target arrangement.)

The test samples that we used for comparative adhesion measurements had rows of spots irradiated with each spot in the row receiving $\sqrt{2}$ more dose than the previous spot. Typically, different rows of spots would have different beam particle and beam energy combinations. By always running one row on each sample with a beam with well known adhesion effects, we always had a control available to check for differences between samples. (See §4.3)

3. Adhesion Measurement

3.1. The Scotch Tape Test

When this project was first started, the assumption was made that a problem as important as adhesion must be very well understood and that many good methods would be available for measuring adhesion. When we started looking for adhesion measuring techniques, we quickly found out that this was not the case. Some tests, such as centrifuge tests, that work for thick films are impractical for thin films; it requires far too great an acceleration to peel a film with a surface density of the order of $50\mu\text{g}/\text{cm}^2$. In fact, the only widespread method for measuring thin film adhesion that we found was the Scotch Tape Test, in which a strip of ordinary adhesive tape is applied to the sample, rubbed into good contact with it and then quickly stripped off. (see Fig. 7.) As we worked more with this method we came to the conclusion that it gives surprisingly repeatable results. By comparing rows that received the same beam, we found that the consistency of the tape test was at least as good as the $\sqrt{2}$ dose ratio between spots. The dividing line between spots that remained after the tape was peeled and spots that were completely removed was quite sharp. Typically, only one spot in a given dose sequence would show partial adhesion. Also, spots near the adhesion threshold do not peel

preferentially at the periphery, which supports the other measurements of dose uniformity.

Since the threshold adhesion, as measured by the tape test, depends weakly on the speed with which the tape is stripped, we always included enough control rows of a well known beam that at the same time any test row was being stripped, a control row was stripped in the same operation. This way, if the speed at which the tape was peeled varied greatly between runs, we could divide the determined threshold on a given run by the error in the apparent threshold in the control row. In practice, changing the speed with which the tape is peeled didn't seem to affect the apparent threshold by more than the $\sqrt{2}$ ratio of beam fluences on different spots on the target, so the worst case error from the speed effect is not very large. However, while the absolute threshold dose for adhesion depends somewhat upon the speed at which tape is peeled, determining ratios of required doses for different beams can be done with quite good accuracy.

3.2. The Loudspeaker Tester

The Scotch Tape test does not give quantitative adhesion measurement; instead, it allows the adhesion to be compared to some fixed strength. This limits the amount of information that is available about the process, so we wanted to find some way to measure adhesion strength that can detect more than one value. Dr. Ricardo Schwarz* suggested that we use a loudspeaker as a linear motor to try to directly measure the amount of force required to pull a known area of material off of the substrate. Since the geometry of a speaker is quite constant, the force should be a very repeatable function of the current in the voice coil at a fixed position of the coil. One problem that was noted with the speaker is that the equilibrium position of the cone shifts from day to day, presumably as the material that supports the speaker cone absorbs water from the air on humid days and releases it on dry days. Therefore, the speaker had to be biased to the equilibrium position before the calibrated currents for testing the samples were applied. If the bias were not used, the shift in equilibrium position would cause the force for a given test

* Private communication. Dr. Schwarz is a visitor in the Division of Engineering and Applied Science at CIT.

current to vary by $\Delta x \times k_{spring}$ where k_{spring} is the spring constant of the support for the speaker cone. (See Fig. 8 for a sketch of the adhesion tester.)

The first big problem with this adhesion tester is attaching the mandrel of the tester to the film under test. We were warned by Dr. Vreeland and Dr. Schwarz that using ordinary glues doesn't work; the stresses developed in the setting of a glue can be very large, and can peel the film before any force is applied externally. The same problem arises in any material that undergoes a phase change (we had thought of freezing something between the mandrel and the film). The expansion or contraction of the material when it changes phase can be enough to peel the film. This left us with one possibility (suggested by Schwarz); a viscous fluid might be used to couple the tester to the film. If the viscosity is high enough, then as long as the testing is done quickly the fluid will act essentially rigidly and will pull the film off. This solves any problems with unintended stresses, since the fluid will relax to relieve any stresses in the system before the sample is tested. Also, if the fluid has a large temperature coefficient of viscosity, it can be cooled down just before testing so that it will have the highest possible viscosity and the longest relaxation time.

One fairly good choice for the fluid seems to be Canada balsam. It has moderate viscosity at room temperature and thickens rapidly as it is cooled to the 0°C. When the mandrel is pulled off of the sample with cooled balsam, the material follows the outline of the mandrel very well. Thus, the area actually pulled off is very repeatable, so the reproducibility should be quite good.

The actual testing of samples proceeded in four steps. First, the speaker was biased to the desired equilibrium position. Then, the mandrel was coated with Canada balsam and pulled away from the plane of the sample. The sample was then placed above the mandrel and the mandrel was pushed into contact with it and held until the balsam was compressed into a very thin film. When the compression phase was done, a short pulse (about 100 msec) of a known current was applied to the speaker. If the sample did not peel, the system was returned to the compression state and then the trial was repeated with a higher current. If the sample did peel, the current was recorded as a measure of the

bond strength. (See Fig. 9 for a timing diagram of the sequence.)

This sequence assured that the fluid film was always in the same state before the sample was tested, and that the force was raised to its calibrated value in a short enough time that the fluid did not relax before the peak force was attained. If the fluid relaxed while the force was at its peak value, the result would be that the mandrel would separate from the film rather than the film from the substrate, so the only part of the run that is required to be quite fast is the risetime of the force. Only runs in which the film separated from the substrate were counted as successful adhesion measurements, since when the film separates from the mandrel, all that has been measured is the strength of the bond created by the balsam layer.

The circuit used to drive the speaker consisted of an opamp wired as an inverting current summer so that the bias could be easily summed into the pulling current and the pushing current applied to the speaker. The pulling current was derived from an LM729 voltage regulator which has very high stability (better than 0.1%) and a precision voltage divider. The pushing current, which required much less critical regulation, was derived from a divider off of the main power supply. The bias current was also derived from an LM729 regulator so that the bias current would remain highly stable over the period of a run. (See Fig. 10 for a block circuit diagram of the speaker driver.)

This equipment is still under development. We have produced no real data with it yet. The mechanical components have all been built, but the electronics are awaiting completion.

4. Discussion of Specific Experiments

4.1. Rutherford Backscattering (RBS) Measurement of the Mixing Depth

The technique of Rutherford Backscattering (RBS) was chosen as a primary method of analyzing samples for this project because of its simplicity and sensitivity. The apparatus can be set up in under an hour with the facilities available at Caltech. The physics of Rutherford scattering, in which a fast projectile ion (typically 1.5 MeV He from a particle accelerator) scatters from a stationary atomic nucleus in a target by pure Coulomb repulsion, is quite well understood and results are easily interpreted. From the ratio of recoil ions to projectile ions, one can compute the total number of atoms of a given species in the target. From the energy of a recoil ion, one can compute from basic kinematics the mass of the target atom which it struck. Also, since the projectile ions lose energy as they pass through a target, one can determine how deep within the target the atom from which it scattered was located. Thus, with relatively simple interpretation, a great deal of information can be extracted from the particles scattered from a target. For an excellent and complete discussion of RBS, see Chu, Mayer and Nicolet (Ch78).

4.1.1. Early Attempts using Low Resolution

This work actually consisted of a number of different attempts to see a mixed layer. Each stage represents an attempt to push the depth resolution of RBS analysis to smaller distances.

The first work was done with gold on fused silica. The sample was irradiated with 20 MeV Cl ions. Since we had no idea how thick the mixed layer might be at first, the sample was first subjected to backscattering analysis with the gold film intact. A 1.5 MeV He beam was used for the backscattering, and a standard Ortec 100 μm silicon surface barrier detector was used to detect the particles. (See Fig. 11 for a diagram of the scattering arrangement.) Figure 12 shows spectra obtained from this work; the top spectrum is from an irradiated area of the sample, the middle spectrum is from an area outside of the beam spot, and the bottom spectrum is the difference. Note that the shape of the gold peak is indistinguishable on and off the beam spot. Since the width of the gold peak is about 10 times the width of the edges, and the gold layer was about 50

nm thick, the depth resolution of this measurement can be assumed to be about 5 nm. Since the result was a null result, a more sensitive method was needed.

Before any more time was spent attempting to measure the thickness of a mixed layer, it was decided that first the presence of such a layer must be verified. To do this, the same sample as in the last experiment was stripped of gold in a dilute aqua regia (HCl:HNO₃:H₂O 3:1:10) solution until no more gold was visible. Then, the sample was analyzed again with RBS, this time to see if any gold at all was detectable on the beam spot. Figure 13 shows the spectra from this. Using standard RBS formulae (Ch78), this represents about $1 \times 10^{13}/\text{cm}^2$ gold implanted in the target. Since the beam dose was about $1 \times 10^{15}/\text{cm}^2$ on this sample, about 1% of the beam dose was mixed into the quartz. This was also tried again with $1 \times 10^{16}/\text{cm}^2$ of Cl, and about $1 \times 10^{14}/\text{cm}^2$ was seen mixed into the quartz, so the 1% figure seems to be reliable. However, this represents such a small amount of mixing that no depth profiling could be done.

The next attempt to measure a mixing layer was on ferrite. Again, no change in the RBS spectrum was apparent when the gold film was still intact on the target. In this case, though, after the gold was etched off, there was no detectable gold remaining mixed into the sample. It is suspected that this is because ferrite, which is a complicated iron bearing ceramic, was probably weakly attacked by the etchant and the layer was removed. (See Fig. 14.)

4.1.2. High Resolution Measurement of Mixing on Ag on Si

The final attempt to measure the thickness of the mixed layer was done with silver on silicon. The target used was a stack of five pairs of silver and silicon, with the silver layers 10 nm thick and the silicon layers 20 nm thick. (See Fig. 15.) The target was prepared entirely in vacuum, so that no oxide layer should be present between the layers. The target was irradiated with about $5 \times 10^{15}/\text{cm}^2$ of 20 MeV Cl. It was then analyzed by Rutherford Backscattering with 1.5 MeV α particles, which were detected with a high quality Ortec surface barrier detector. The measured resolution of the system for α 's scattered from gold was 22 keV FWHM. (See Fig. 16.) Thus, σ_E , the energy standard deviation, is about 10 keV for the system. The target was enclosed in an aluminum shroud in thermal contact

with a liquid nitrogen bath to minimize the buildup of carbon on the target during the backscattering. The pressure in the chamber during the analysis was below 1×10^{-6} Torr. No carbon buildup was seen on the target during the backscattering runs; however, since the Cl irradiation was done without the cryoshield, about $1 \mu\text{g}/\text{cm}^2$ of carbon was deposited on the beam spot (as measured by RBS). This made a very convenient marker on the target so that one could tell whether the area being analyzed was on or off of the beam spot. It also introduced a 1.5 keV shift in the energy of the edges because of its dE/dx . (See Figs. 17 and 18.)

Since dE/dx for α particles silver is about 600 eV/nm, to see a 2 nm mixed layer, the width of the boundary between layers must be determined to 1.2 keV. This requires careful fitting of the shape of the edges since the needed energy resolution was 8 times less than σ_E . This was accomplished by least-squares fitting a curve of the form

$$Y = A + Bx + C \exp\left(-\frac{(x-\mu)^2}{2\sigma^2}\right)$$

to the high energy edge of the topmost silver layer (which was underneath the first silicon layer). Table 2 shows the data from this work. All of the spots measured on the target had edge widths within 0.1 analyzer channel (about 300 eV) from the central value of 3.13 ± 0.05 channels. The sensitivity of χ^2 to the width was very good: changing the width by 0.05 channel increased χ^2 by about 50%, so the fit should be reliable to at least 0.1 channel.

Now, from the calculations done below Table 2, $\Delta\sigma_{tot}$ for data taken on the beam spot versus data taken off the beam spot is .033 channels. Since $\sigma_{system} \cong 3.1$ channels, the minimum detectable change in the width of the peak would be

$$\Delta\sigma = \left((3.1)^2 - (3.1 - .033)^2 \right)^{1/2} \cong .45 \text{ channels} \cong 1.4 \text{ keV}$$

which corresponds to a mixing depth of about 2.3 nm. At this level, nothing was seen since the difference between the widths on and off the spot were well inside of the 1 σ limit.

Thus, the result of using RBS to determine the mixing depth is still null. If any mixing is occurring, it is probably on a scale of less than 2 nm, which is not practical to measure by RBS techniques, so in the future, some other method will be needed if further analysis of the

interface is to be done.

4.2. Electron Diffraction and TEM Analysis

In the case of silver on silicon, compounds are only known to form under very unusual conditions. Thus, this system is ideal for searching for new mixing processes since already known processes (such as thermal heating, low energy mixing etc.) are known not to cause any new crystalline compounds to form. For this work, we prepared samples as in §2. Then, the samples were etched in HNO_3 to remove the silver layer on top. After the silver layer was removed, the samples were jet etched from the back with an HF and HNO_3 mixture until the sample was etched through. (See Fig. 19.) The material very near the hole formed a very thin edge which could then be studied with TEM and electron diffraction. The results were fairly spotty; in some cases patches about 10 nm across of crystal regrowth were seen, but these patches only occurred on a few samples. At first, it was thought that these patches could have been AgSi_2 but further looking around revealed that AgO_2 would have exactly the same crystal structure and very nearly the same lattice constants, and since this is a fairly well known compound, we assume that this is what was being seen. In any case, since all of the samples showed excellent adhesion, and only a few showed this crystal growth, and even then it only covered some of the sample, it is fairly clear that the presence of this structure is not directly related to adhesion. (See We82 for details.)

4.3. Dependence of Threshold Adhesion on dE/dx

Knowing the dependence of adhesion on dE/dx is very important; any theory that tries to predict adhesion needs to reproduce this function correctly. Also, knowing if it is the same function on all materials determines if the adhesion problem is one or many. If the original theory of Griffith and Qiu were correct, one would expect the adhesion to behave as something like $(dE/dx)^4$ since this is approximately the way sputtering of dielectrics behaves (Me82). If the process is very different from this, it might manifest this difference in its dependence on dE/dx .

The first dE/dx dependence measurements were done on the gold on tantalum system. The samples were prepared as described in §2. Gold on tantalum was chosen for this measurement for a number of reasons.

First, the beam dose required is quite small, so that the time required to collect a large number of data points is not prohibitive. (See Fig. 20.) Second, gold on tantalum seems to be one of the easiest systems on which to get highly repeatable results; the Scotch Tape test can be reproduced to about 20% without any difficulty. The irradiations were done with 20 MeV Cl, 7.2 MeV Cl, 3.2 MeV Cl, 12 MeV F, 1 MeV H, 1 MeV He, 87 MeV Ar, and 107 MeV Kr. The dE/dx values for these beams came from Northcliffe & Schilling (No70) except for the H and He values, which came from Zeigler (Ze77 & An77). Fig. 21 is a plot of threshold dose *vs.* dE/dx with a least squares fit which gives $\text{Dose}=(dE/dx)^{-1.6\pm 0.2}$

The other dE/dx dependence measurement done was with gold on fused silica. The work was done in the same manner as for gold on tantalum, but we discovered that ions lighter than Cl did not have sufficient dE/dx to induce any measurable adhesion. Thus, in this case, the dependence does not appear to be a power law at all, but contains a threshold dE/dx . Since beams heavier than Cl other than Kr are hard to obtain, we have only two points for the adhesion *vs.* dE/dx , which makes it quite difficult to draw any real conclusions about the form of the curve especially since the uncertainties in the Kr dose are large.

5. Discussion of Mechanisms

In the introduction, a number of possible mechanisms for the improvement of adhesion by ion beam bombardment were very briefly mentioned. In this section, I will discuss these mechanisms in more detail, and will explain why it is thought that each of these is not reasonable. So far, a plausible mechanism which has sufficient detail to be predictive has not been proposed for high energy heavy ion induced adhesion.

5.1. Nuclear Collision Driven Mixing

This mechanism would be a simple way of inducing adhesion. It is the mechanism seen in low energy (*i.e.* nuclear stopping power region, $E < 100$ keV/nucleon) ion induced adhesion. This mechanism relies on direct beam-lattice atom collisions. The beam particle mass is comparable to the target atom mass, so target atoms receive a large fraction of the beam energy, and are scattered through large distances in the target. This gives rise to very long range mixing (tens of nm) and does severe damage to the lattice of the bombarded material.

The occurrence of this mechanism would have been indicated by a number of obvious results. First, the mixed layer would have been clearly seen by Rutherford backscattering. Second, the dependence of adhesion on beam energy would have been very different. At high energy, nuclear stopping power falls off quickly, so one would expect this mechanism to become weaker and weaker at higher energies. Instead, as the beam energy is increased, the adhesion increases, at least up to the energy at which the electronic stopping power reaches its peak at about 1 MeV/amu. Third, high energy ion beam induced adhesion is effective on systems such as silver on silicon where low energy ion beams have not been observed to induce adhesion.* Also, low energy ion beams require a much higher dose ($\gtrsim 1 \times 10^{16}$ /cm²) than is needed in the high energy case.

* Dr. B. X. Liu, personal communication while he was a visitor at Caltech from Qinghua University, Beijing, PRC.

5.2. Thermalized Ion Explosion Driven Adhesion

This mechanism depends on the occurrence of the process described by Seiberling (Se82) for the sputtering of dielectrics. Briefly, what occurs is that in a dielectric, where the electronic relaxation time is long ($\lesssim 1 \times 10^{-12}$ sec), the positively charged region created along the beam ion path as a result of electron scattering by the beam is sufficiently long lived that the electrostatic repulsion of the lattice ions can transfer energy to them. They then thermalize so that a hot plasma is formed along the beam path. This plasma has temperatures of typically 5000K. Griffith (Gr82) proposed that this plasma could eject some material at the interface of the materials, thus causing mixing and adhesion. Since the thermal energy distribution of the ions in the plasma falls off very quickly at high energy, very little long range mixing would be expected because few ions would have sufficient energy to travel far through the solid lattice.

This mechanism would have one very obvious signature if it were responsible for the adhesion observed: it would occur only when one of the materials involved is a dielectric. In a metal, where electronic relaxation times are of the order of 1×10^{-15} seconds there is not sufficient time to convert the electrostatic energy along the beam ion path into kinetic energy of the ions. In particular,

$$E = \frac{p^2}{2m} = \frac{(F \times \Delta t)^2}{2m} = \frac{Z^4 e^4 c^2 (\Delta t)^2}{2R_0^4 m c^2}$$

where E is the transferred energy, R_0 is the lattice spacing, m is the ion mass, e is the electronic charge, and Z is the ion charge (in units of e). Now, $e^2 \cong 1.4$ eV-nm, $c \cong 3 \times 10^{17}$ nm/sec, and for typical lattice ions (assuming that mainly the conduction band electrons will be scattered), $Z \cong 1$, $m c^2 \cong 1 \times 10^{11}$ eV and $R_0 \cong 0.2$ nm, so

$$E \text{ (in eV)} \cong \frac{1^4 \times (3 \times 10^{17})^2 \times 1.4^2 \times (\Delta t)^2}{2 \times 0.2^4 \times 1 \times 10^{11}} \cong 5.5 \times 10^{26} \times (\Delta t)^2$$

Now, in highly conducting materials, the electrons remain away from the ion track for a time comparable to $\frac{2\pi}{\omega_p}$ where ω_p is the plasma frequency of the electrons in the material and is of the order of $1 \times 10^{16} \text{sec}^{-1}$ (Sa71). Thus, $\Delta t \cong 1 \times 10^{-15}$, so $E = 6 \times 10^{-4}$ eV so the ion pair receives an energy

much less than the lattice binding energy. Thus, there is not enough energy to disrupt the lattice so this mechanism should be very weak in highly conducting materials.

This conflicts badly with the experimental evidence that, in fact, conducting materials are as easy or easier to bond than dielectrics. The one remaining possibility was that all the materials we used had an overlying layer of dielectric that was mediating the adhesion. Since many materials do form oxides on the surface that are insulating, this looked like a promising possibility. However, silicon, for example, (see §6.1) behaved very differently from its oxide. Also, even in the case where oxides grow on such surfaces, they tend to be very thin, usually much less than 1 nm. Thus, the thermal and electrical properties of such a layer are quite different than those of the bulk material and it is not expected to exhibit enhanced dielectric sputtering. Also, the silver on silicon sample from China Lake which was produced under UHV conditions should be free of any intervening oxide layer, and yet it shows quite good adhesion enhancement.

6. Random Observations about Samples

This section summarizes quite a few observations that were made concerning the various materials used in this project. There is no attempt to include hard data or to study in depth the result presented here. They were observations made in passing, and need to be studied in detail in the future. These comments may also serve to alert people working with these materials to possible behavior that might not be expected.

6.1. Behavior of Silicon with Different Cleaning Procedures

Because the silver on silicon system has received so much study, a number of interesting properties have been noticed about it. As in any problem of surface physics, the cleanliness of the surface under study is quite important. Because of this, we have tried different cleaning procedures as recommended by people who work with silicon. We soon found out that the residual adhesion on a sample depends (not surprisingly) quite strongly on the cleaning given the sample before the film is deposited. The usual cleaning procedure for silicon, which ended with a rinse in reagent grade methanol, produced very low residual adhesion of silver films and moderate residual adhesion of gold films. However, if the methanol rinse is omitted, fairly high residual adhesion is seen in silver films and very high residual adhesion is seen with gold films. In fact, with gold films, the bonding is sufficiently good before irradiation that the film withstands even the most determined scrubbing. This clearly points to the importance of knowing the condition of a surface before bonding is attempted. What makes this behavior interesting is that it is not consistent with the (supposedly) well understood surface on a piece of freshly etched silicon. Silicon is expected to have a few monolayers of oxide grown on the surface after cleaning, so the residual adhesion of films on silicon should be like that of films on SiO_2 . However, gold shows very weak residual adhesion on SiO_2 , while silver shows extremely good residual adhesion on SiO_2 . Thus, the methanol rinsed Si surface acts like it has an oxide layer for gold, while the freshly etched surface acts like an oxide for Ag films. This probably indicates that some layer other than oxide overlies the Si surface, but what it might be is not clear.

6.2. Enhanced Adhesion and Wettability

This is another quirk that was noted on Si, probably because Si has been studied more than almost anything else. I noticed this when I was removing the metal film from the surface of an irradiated Ag on Si sample. First, the sample was etched in dilute HNO_3 to remove the silver from the surface. Then, it was etched in $\text{HF}:\text{H}_2\text{O}$ 1:1 to remove any oxide layer that might have grown on parts of the sample not covered by silver. What remained was an apparently featureless piece of silicon (no beam spot was visible). However, when the sample was rinsed in methanol, I noted that the area where the beam spot had been was much more wettable than the unirradiated area. This was manifest in the methanol remaining on the beam spot after the film had beaded off the rest of the sample. After I noticed this, I decided to try to see if the difference in the sample extended in any significant distance, or if it was entirely on the surface. I briefly etched the sample in $\text{HF}:\text{HNO}_3:\text{H}_2\text{O}$ 100:1:100 (approximately) to remove a little bit of silicon. After the etching, the wettability was still very apparent, so the modified silicon was not just on the surface where some chemistry with the silver film (or a dirt layer) could have modified it.

The first idea that was considered when this effect was seen was that the surface had been roughened by having tracks etched into it (even though tracks had never been seen on silicon). However, when SEM photos of the sample were taken, the irradiated and unirradiated areas looked exactly the same. No macroscopic damage had been done to the silicon that could be etched sufficiently to make it visible at the 1 level. However, this is not necessary to affect wetting; a change in the surface monolayer of a material is sufficient to change its wettability.

This result presents an interesting problem: while there is no known mechanism by which high energy heavy ions can produce bulk damage to a highly conducting material like $10 \Omega\text{-cm}$ silicon, there is evidence that such damage must be occurring. Some process, which may or may not be linked to adhesion, is taking place. In a way, the wettability in itself is an adhesion problem, using a liquid instead of a solid film on the surface. The big difference is that this is *post facto* adhesion. The material is being applied after irradiation instead of before. At some time, it would be interesting to try this with solid films. However, it is much more

difficult in the case since there is the problem of contamination occurring between the irradiation and the film deposition, unless the entire process occurs in a single operation in a UHV chamber. The liquid system was inherently contamination free since the sample could be tested within a fraction of a second of its etching.

Further experimentation has shown that this wettability difference also arises on tantalum. In this case, the sample was etched for about half an hour in 1% NaCN solution to remove the gold layer. The tantalum was then rinsed in methanol and showed significantly improved wettability on the beam spots. The sample was then dipped briefly in HF:H₂O 1:1 to etch a little tantalum off the surface. The effect was then even more apparent. However, more repetitions of the same process on the same sample failed to show the effect. Presumably, the damaged layer had been etched off by the HF.

When gold on quartz samples are etched in NaCN to remove the gold layer, no improved wettability is seen. This was quite interesting because quartz is the only one of the three materials tested where such an effect could have been reasonably expected since it does show track damage from high energy heavy ion beams.

6.3. Electrical Contact Properties of Metals on Semiconductors

Since one of the most important uses of thin films is in the electronic industry, where they are used to make electrical contacts to semiconductors, we decided to look at the electrical properties of metal-semiconductor junctions before and after irradiation. We also hoped that the changes in junction properties might lead us to some understanding of the mechanism involved in adhesion.

We prepared samples of Au on GaAs, Au on Si and Ag on Si. When we irradiated them, we found that the contacts changed from being very good diodes (1000:1 ratio of forward to reverse current) to being fairly close to ohmic (2:1 ratio). However, this transition occurred at very low beam doses. Only about $1 \times 10^{12} / \text{cm}^2$ of 20 MeV Cl were sufficient that any more irradiated caused little further change in the junction properties.

When we found out that the dose required to modify the properties of a contact was so different than the dose required for adhesion, we concluded that the two phenomena probably have different origins, so we

delayed further work on this project until more time and assistance is available. Thus, we have very little detailed data about junction properties. However, the rough information we have will provide a good starting point for a detailed study of this, which might be of interest to semiconductor manufacturers who need to make ohmic contacts to materials and to people preparing electronics to fly in space, where cosmic rays might do permanent damage to semiconductor junctions.

6.4. Damage to Compound Semiconductors

Another effect that we noticed when working with adhesion on semiconductors was that high energy heavy ion beams do much more damage to some materials than expected. In compound semiconductors such as GaAs and InP, we found that even when the resistivity is very low $\rho \cong .001\Omega\text{-cm}$, the crystal structure can be completely disrupted by heavy ion beams. In one GaAs sample which we had analyzed by x-ray scattering, the beam spot was quite clearly visible. So far, there is no evidence that such severe damage occurs in Silicon (although some might be occurring; see §6.2.). However, the compound semiconductors are much softer and weaker than Si (which is extremely hard and strong), so they might be reasonably expected to be much more sensitive to damage than Si. We have also done some preliminary measurements of the sputtering yield of InP. It seems to show significantly enhanced sputtering over the predicted Sigmund yield. Thus, there may be evidence that other processes for transferring energy from electrons to the lattice than the Watson-Tombrello dielectric process (Wa82) exist.

7. Conclusions

The first and probably most important result of this project is that a method for bonding an enormous variety of materials has been found. So far, no combination of materials has been found that cannot be made to adhere. There are some materials that are unsuitable for use in this technique, though. Certain materials, such as I-carbon films, seem to decompose under irradiation. Also, organic polymers are easily damaged by radiation, but since they require a very low dose to cause adhesion, the technique may yet be practical. In semiconductor systems, the usefulness has not been fully determined. Very good adhesion can be obtained

with relatively moderate doses, and very low resistance electrical contacts are formed under the adhered areas. However, most semiconductors are very sensitive to radiation damage, so that the areas where enhanced adhesion is desired cannot overlay active areas of the semiconductor. However, this should not limit the usefulness of the technique for making electrical contacts around the periphery of the active area. It appears that optical equipment should be a very good area in which to apply this method. Thin films can be bonded to substrates with only very minor changes in the optical properties of the system. The thin mixing layer formed by this method should make it useful even on multilayer dielectric optical films since the disturbance to the layers is minimal. Also, the layers are not sputtered very much by the beam. The other very promising application for this is in metal on metal systems. The doses required for excellent adhesion are extremely low, so samples can be bonded quickly and easily. Since only a minimal amount of beam is implanted into the substrate, and since high energy ions do very little damage to metals until they have nearly stopped, this method should be useful even in critical cases where the bulk properties of the substrate are important.

There is, obviously, room for a lot more study in this area. So far, very little is understood about the mechanism of the adhesion. The $(dE/dx)^{-1.6}$ rule found for beam dose *vs.* adhesion threshold on metal-metal systems is not understood. A high energy heavy ion such as 20 MeV Cl deposits of the order of 1 keV/lattice spacing in the electrons of a typical solid, and they are scattered over ranges as great as 5 nm, so there is plenty of energy available to do substantial rearrangement of electrons. Thus, it is expected that the mechanism will primarily involve rearrangement of electronic states near the interface of the materials. The difficulty in studying the details of the mechanism is that there are not many good techniques for examining what changes in the electronic structure are taking place.

Even on dielectrics, where originally it was thought that the mechanism would be in some simple way tied to sputtering, it doesn't look so easy. The abrupt threshold of adhesion as dE/dx varies indicates that the process is not easily tied to sputtering, where the yield behaves approximately as $(dE/dx)^4$, which would allow 12 MeV F to cause

adhesion relatively easily.

To further study the mechanism involved in adhesion presents a real challenge. Surface techniques such as ESCA (Electron Scattering for Chemical Analysis) are not useful below the top few layers of a material. However, the possibility of making very thin films that can be penetrated by an ESCA probe exists. We have received some 5 nm Au on SiO₂ films from IBM which were deposited at 77K so that, according to the people who made them, the film is continuous (rather than in islands, as is typical of very thin films). The ESCA probe would allow the energy levels of the electrons at the interface to be studied by looking for scattering resonances where bombarding electrons have just sufficient energy to excite a bound electron in the material. A knowledge of the electronic states at the surface might allow the reconstruction of the process involved in the actual adhesion.

Since adhesion is by definition something that takes place at an interface between two materials, it is not able to be studied by normal surface techniques. Methods that are particularly effective at studying processes deep within a sample do not have the sensitivity or depth resolution needed to probe the details of the very thin region in which the adhesion is actually taking place. Until techniques with sufficiently good resolution become available, the process will have to continue to be analyzed primarily from a macroscopic point of view. Any proposed mechanism will have to be matched primarily to the dependence of adhesion strength on dose and dE/dx along with the mechanical properties of the materials.

Table 1
Material Combinations Tested
for
High Energy Heavy Ion Induced
Enhanced Adhesion

Table 1 lists the various substrate, film and beam combinations we have tested for enhanced adhesion. In the dose column, numbers preceded by \cong or \lesssim have been measured using movable slits to define the beam shape, so the actual dose is not well known. Numbers preceded by $<$ have been tested at the dose shown, and show adhesion, but lower doses have not been tried so the threshold may be much lower. Numbers without any prefix represent values measured as described in §4.3 and should be reliable to $\sqrt{2}$. All numbers represent the dose required to pass the "Scotch Tape" test.

| Substrate | Film | Beam | Dose (#/cm ²) | Comments |
|--------------------|------|------------|------------------------------|--|
| Si, n-type 10 Ω-cm | Au | 20 MeV Cl | ≈5×10 ¹⁴ | Residual adhesion is very good. Unirradiated samples often pass tape test. |
| | Ag | 20 MeV Cl | ≈2×10 ¹⁵ | Very low residual adhesion except when sample not rinsed in methanol after HF dip. Then, residual adhesion is near the tape threshold. |
| Ta | Au | 107 MeV Kr | 5×10 ¹² | * |
| | Au | 87 MeV Ar | 2.8×10 ¹³ | * |
| | Au | 27 MeV Ar | 2×10 ¹³ | * |
| | Au | 20 MeV Cl | 2.5×10 ¹³ | |
| | Au | 7.2 MeV Cl | 4.5×10 ¹³ | |
| | Au | 3.2 MeV Cl | 9×10 ¹³ | |
| | Au | 12 MeV F | 7×10 ¹³ | |
| | Au | 3.7 MeV F | 1.3×10 ¹⁴ | |
| | Au | 35 MeV O | 1×10 ¹⁴ | * |
| | Au | 1 MeV He | 6×10 ¹⁵ | |
| | Au | 1 MeV H | 3×10 ¹⁶ | Peak adhesion is very weak. Very little material is left after the tape test, but there seems to be a real threshold for none <i>vs.</i> what little remains |
| | Ag | 20 MeV Cl | ≤1×10 ¹⁴ | |

* Berkeley runs, listed doses adjusted down from measured value by 0.5 to bring 27 MeV Ar point into line with CIT data.

Table 1
(cont'd)

| Substrate | Film | Beam | Dose (#/cm ²) | Comments |
|---|------|------------|------------------------------|--|
| | Au | 107 MeV Kr | 1.5×10^{13} | * |
| | Au | 20 MeV Cl | 5×10^{14} | |
| Fused SiO ₂ | Au | 12 MeV F | $> 5 \times 10^{10}$ | No adhesion observed with 12 MeV F beam. |
| | Au | 27 MeV Ar | $\approx 3 \times 10^{14}$ | |
| | Ag | 20 MeV Cl | $< 2 \times 10^{14}$ | |
| InP p-type .001 Ω-cm | Au | 20 MeV Cl | $< 5 \times 10^{14}$ | |
| GaAs, heavily doped | Au | 20 MeV Cl | $\leq 1 \times 10^{14}$ | |
| W | Au | 20 MeV Cl | $< 1 \times 10^{14}$ | |
| Teflon [®] | Au | 1 MeV H | $\approx 3 \times 10^{13}$ | Higher doses burn substrate |
| Polytetrafluoroethylene | Au | 1 MeV He | $\leq 1 \times 10^{14}$ | |
| Topaz Al ₂ SiO ₃ (OH,F) ₂ | Au | 20 MeV Cl | $\approx 5 \times 10^{15}$ | |
| | Pd | 20 MeV Cl | $< 1 \times 10^{15}$ | |
| Al ₂ O ₃ | Ag | 20 MeV Cl | $\leq 5 \times 10^{15}$ | |
| Alumina/Silica/ Magnesia Glass-Ceramic | Cu | 20 MeV Cl | $\leq 3 \times 10^{15}$ | |
| Ferrite | Au | 20 MeV Cl | $\approx 1 \times 10^{15}$ | |
| I-Carbon (See §2.1.4) | Ag | 20 MeV Cl | $\approx 1 \times 10^{15}$ | These films seem to decompose under irradiation. The adhesion was at best weak, and where the metal peeled, the I-carbon had turned dark brown underneath. I suspect that the films were reverting to graphite (as diamond is wont to do). |

Table 2
 Curve Fit Results
 from
 Mixing Depth Measurement
 of
 Ag on Si Multilayer Target
 (See §4.1.2)

Table 2 shows the curve fit parameters from the high edge of the Ag peak from the target described in §4.1.2. The value of χ^2 is clearly much worse than that expected from a perfect fit, but one does not really expect a detector spectrum to give a perfect Gaussian, and the deviation is actually quite small. The uncertainties used to derive χ^2 were just the \sqrt{n} counting statistics, and since n is of the order of 30000 counts per channel, a $\frac{1}{2}\%$ deviation from a perfect Gaussian could double χ^2 .

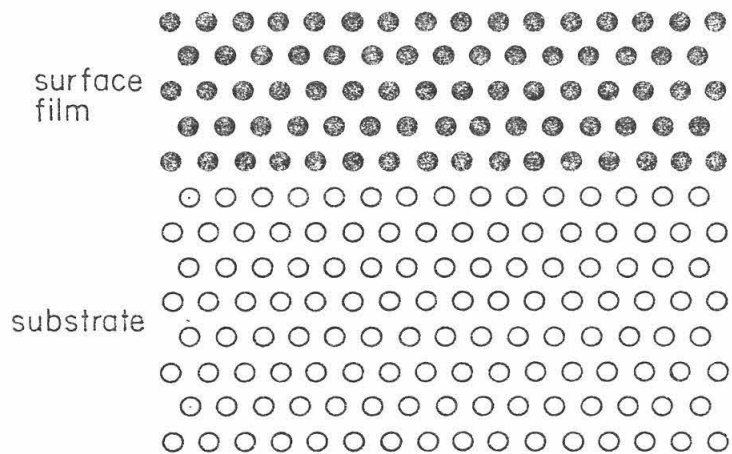
| Run | Ag counts (LT corrected) | μ (channel) | σ (channels) | χ^2 (15 DF) | Comments |
|-----|-----------------------------|--------------------|------------------------|---------------------|----------|
| 3 | 1.247×10^6 | 414.88 | 3.10 | 21 | off spot |
| 4 | 1.256×10^6 | 414.94 | 3.12 | 15 | off spot |
| 5 | 1.243×10^6 | 414.96 | 3.21 | 33 | off spot |
| 6 | 1.240×10^6 | 414.28 | 3.14 | 12 | on spot |
| 7 | 1.240×10^6 | 413.90 | 3.05 | 10 | on spot |
| 8 | 1.246×10^6 | 414.36 | 3.16 | 19 | on spot |
| 9 | 1.248×10^6 | 415.08 | 3.18 | 29 | off spot |
| 10 | 1.250×10^6 | 415.36 | 3.12 | 21 | off spot |

Thus, off the beam spot, $\langle\sigma\rangle=3.15 \pm .042$. When the standard deviation of the mean is used, $\langle\sigma\rangle=3.15 \pm .019$. On the beam spot, $\langle\sigma\rangle=3.12 \pm .047$, or, using the standard deviation of the mean, $\langle\sigma\rangle=3.12 \pm .027$. Then, the uncertainty on the difference in the means is $\Delta\sigma_{tot} = (\Delta\sigma_{on}^2 + \Delta\sigma_{off}^2)^{\frac{1}{2}} = .033$ channels

Figure 1
Effect of Low Energy Ion Mixing
(see §1.1)

- a) Schematic of substrate lattice with thin film lattice on top before low energy ion irradiation is done. Both the surface film and the substrate can be made of any resistivity material, since low energy mixing does not depend on electronic stopping power.
- b) After the low energy ion bombardment is complete, the surface has been sputtered away by Sigmund sputtering. The materials are mixed with a mixing depth of the order of tens of nm. The mixing depth is quite large because lattice ions receive very large energies from direct collisions with the beam ions, giving them a long range in the material. The beam particles are implanted within 100 nm of the surface of the film, and the lattice structure of both the film and the substrate is disrupted. The amount of beam implanted is $\gtrsim 1 \times 10^{17} / \text{cm}^2$.

a) Before irradiation



- substrate atom
- thin film atom
- ⊗ beam atom

b) After irradiation

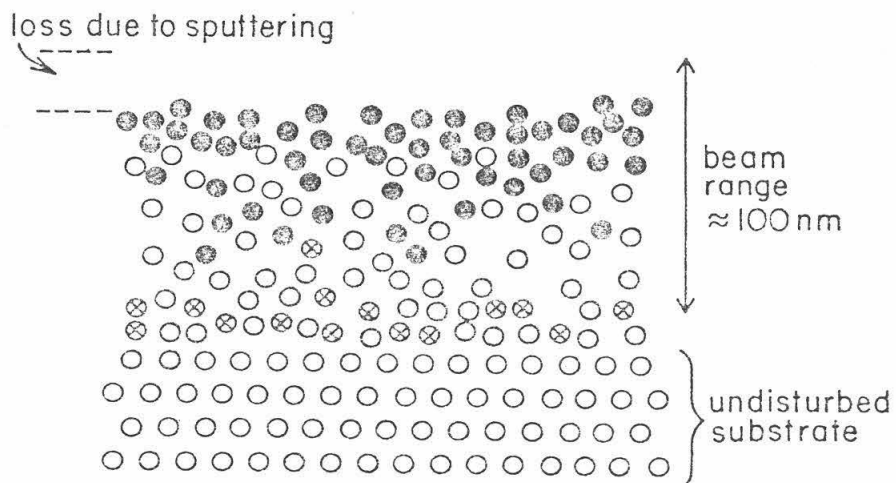


Figure 2
Griffith Model
for
High Energy Heavy Ion Induced Adhesion (Gr82)
(see §1.2)

- a) Unirradiated Lattice. In the rest of the figure, the film is assumed to be an electrical conductor and the substrate is a dielectric.
- b) This shows the effect of a single beam particle on the lattice. The metal film is not disrupted because the beam is depositing energy only in the electrons of the material. In the dielectric substrate, a hot ($\cong 5000\text{K}$) plasma is formed, as in the Seiberling model of dielectric sputtering. Atoms of the dielectric are ejected by the hot plasma which mixes the substrate with the film. The mixing layer is thin because the ions in the dielectric have a thermal distribution, which falls off exponentially at high energy, so few ions have large enough energies to travel far from their initial positions. The beam ion comes to rest about $5\mu\text{m}$ from the surface of the film. Since the sputtering yield of metals with high energy ions is very low, no metal is removed from the surface.
- c) When the irradiation is done, a thin layer ($\cong 1\text{nm}$) will be mixed at the interface. The metal is not significantly disturbed. The dielectric lattice is damaged to a depth of about about $5\mu\text{m}$. About $1 \times 10^{15}/\text{cm}^2$ of beam is implanted at this depth, which is about 100 times less than is needed for low energy ion mixing and is much deeper than the implantation depth for a low energy ion mixed system.

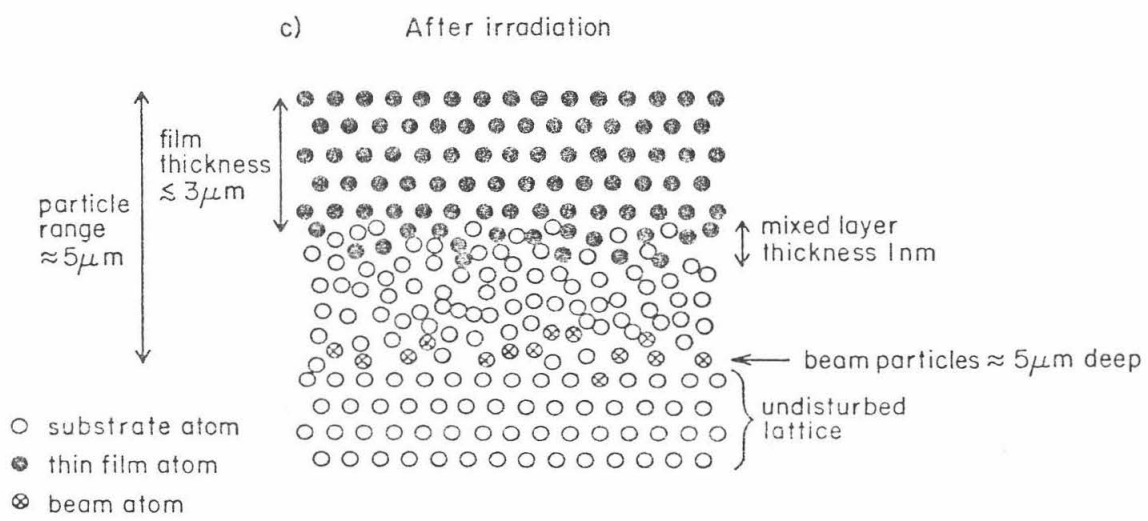
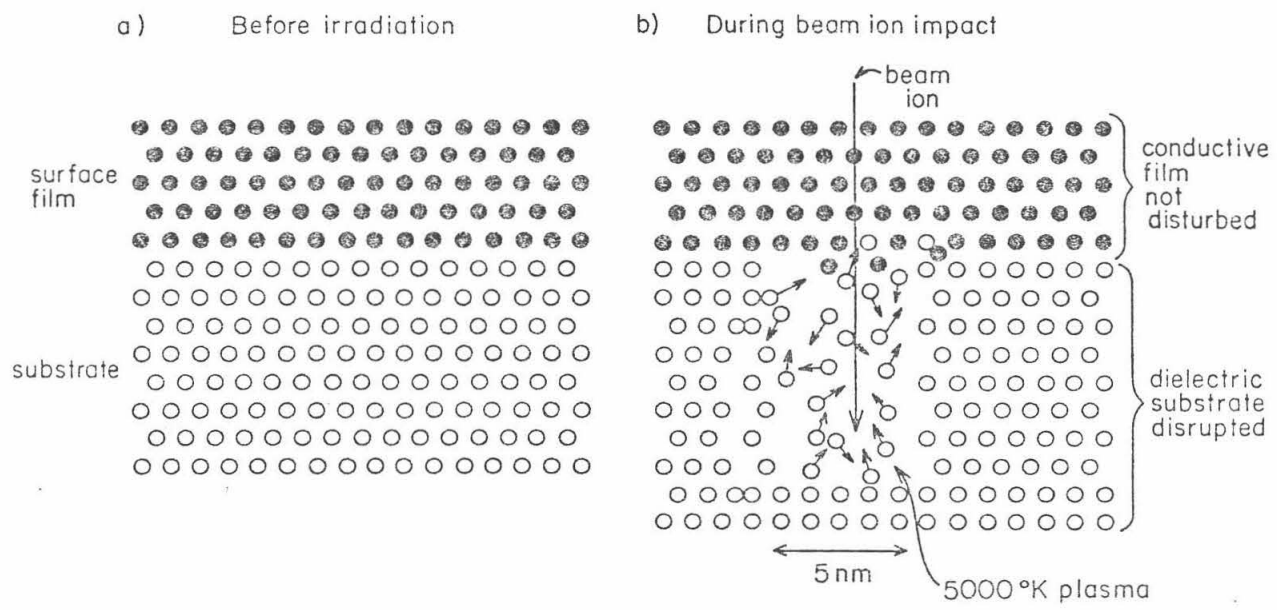


Figure 3
Comparison of Energy Spectra
of
Particles Displaced by a Low Energy Ion Beam
vs.
Particles Displaced by a High Energy Ion Beam
(see §1.2)

This plot compares the energy spectra of particles scattered during a low energy ion impact on a surface to that of a high energy ion impact. The solid line is the spectrum generated by a high energy (electronic stopping power) impact; its shape is the Maxwell-Boltzmann with $k_b T = 0.5$ eV or $T \cong 6000K$

$$N(E) = E^{\frac{1}{2}} e^{\frac{-E}{k_b T}}$$

or, including the Jacobian for $\log E$,

$$N(\log(E)) = E^{\frac{3}{2}} e^{\frac{-E}{k_b T}}$$

Note the extremely rapid falloff of this distribution at high energy. The dashed line is

$$N(E) = E^{-2}$$

or

$$N(\log(E)) = E^{-1}$$

which is the appropriate spectrum for a low energy ion impact. Note that it falls off very weakly at high energy.

Fig. 3 Comparison of Energy Spectra

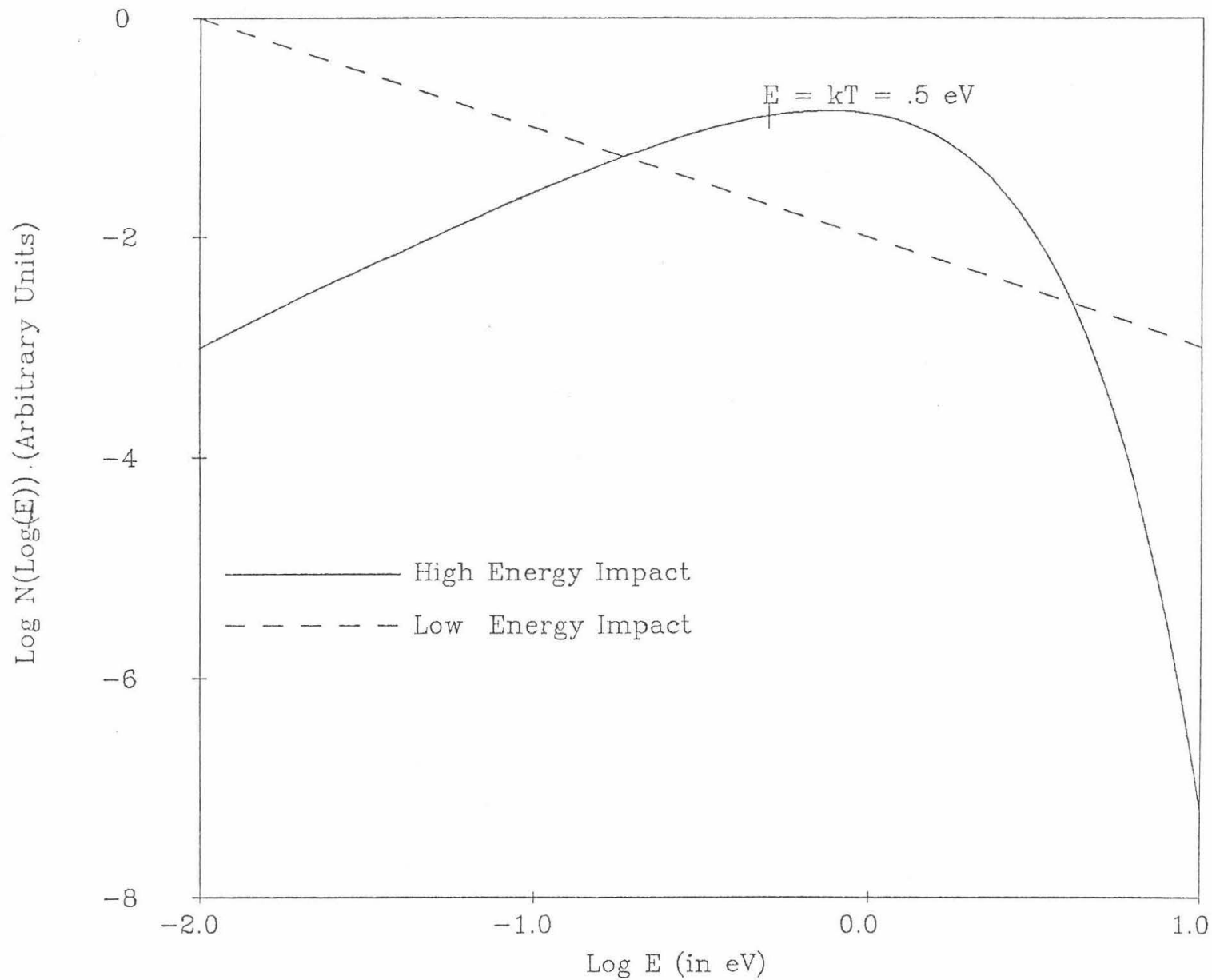


Figure 4
Photographs of Various Bonded Samples
(see §1.2)

Top: Samples labelled 1 and 2 are Au on GaAs and Au on InP, irradiated through a metal mask with small holes in it to limit where the beam strikes the sample. They were then stripped with tape, leaving the gold pattern bonded to the substrate. The spots are about $200\ \mu\text{m}$ in diameter. Sample 3 is Au on Ta, irradiated through slits and stripped with tape.

Bottom: This is a sample of Si with 50 nm of Au on top. It was irradiated with 20 MeV Cl, then stripped with tape. After it was stripped, the adhesion was further tested by soldering a wire to the gold film with conventional solder and a soldering iron. The wire is quite strongly attached, indicating that adhesion is not destroyed by thermal cycling.

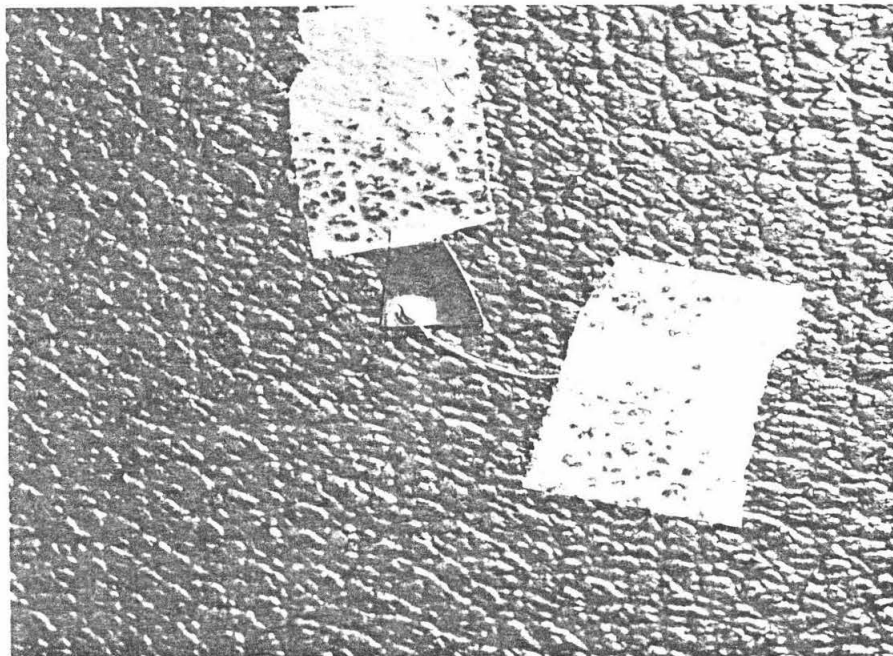
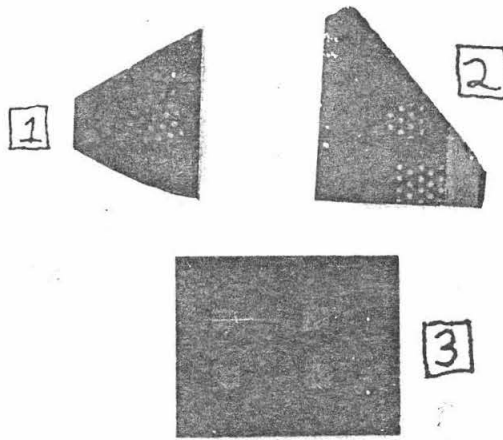


Figure 5
Target Setup for Sample Irradiation
on the
Caltech ONR-CIT EN Tandem
(see §2.2)

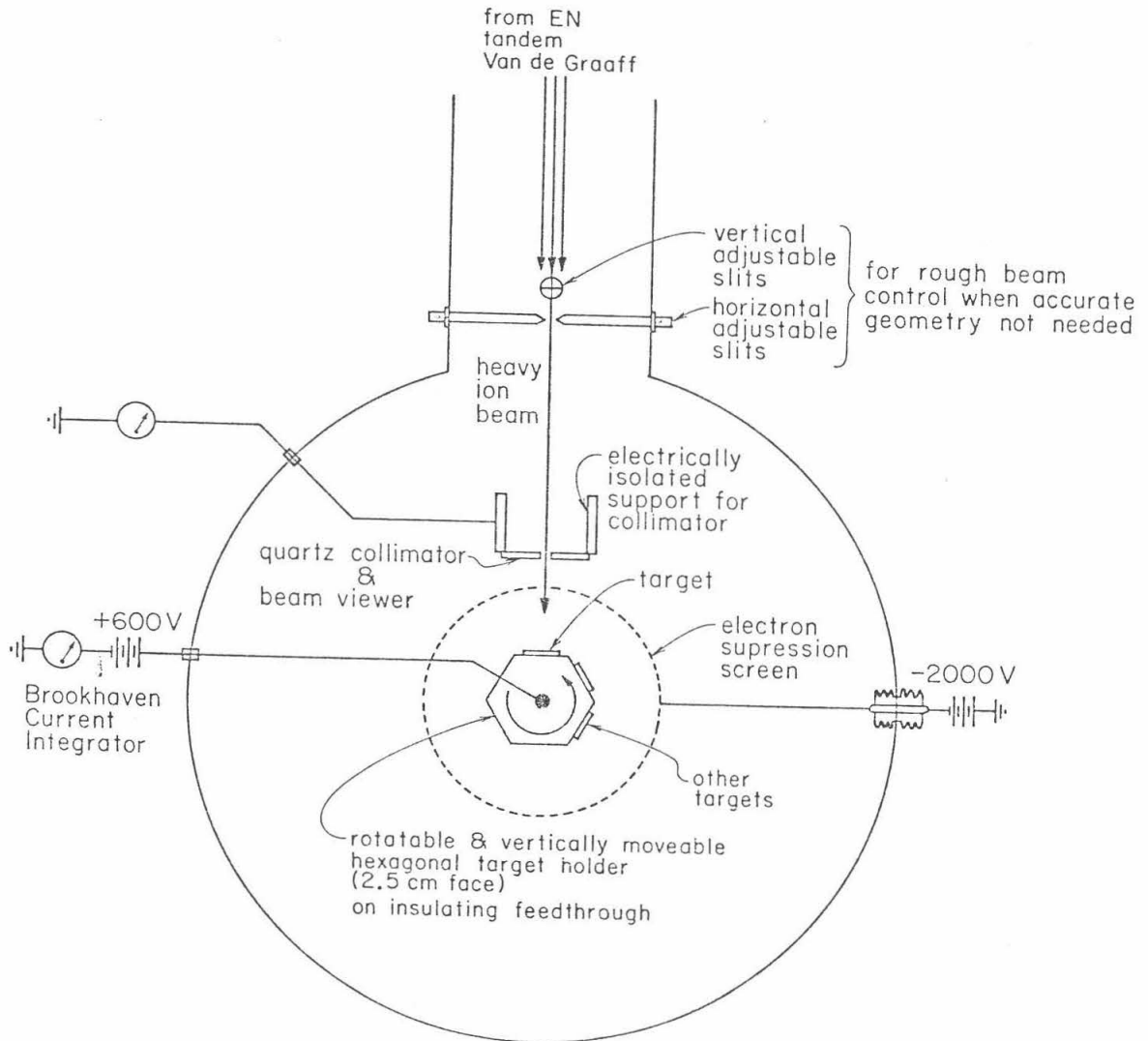


Figure 6
Target Setup for Sample Irradiation
on the
LBL 88" Cyclotron
(see §2.2)

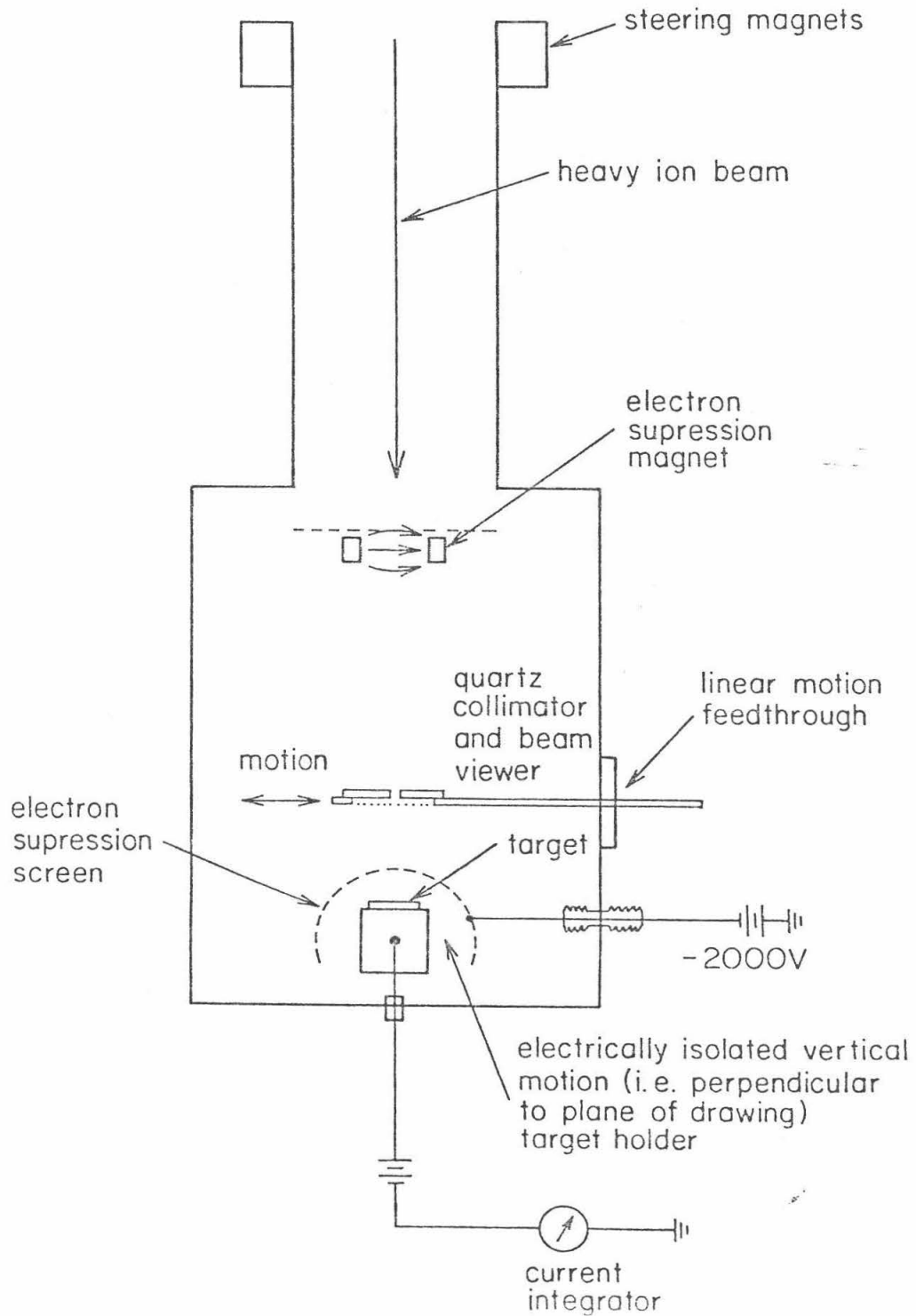


Figure 7
Schematic of "Scotch Tape" Adhesion Test
(see §3.1)

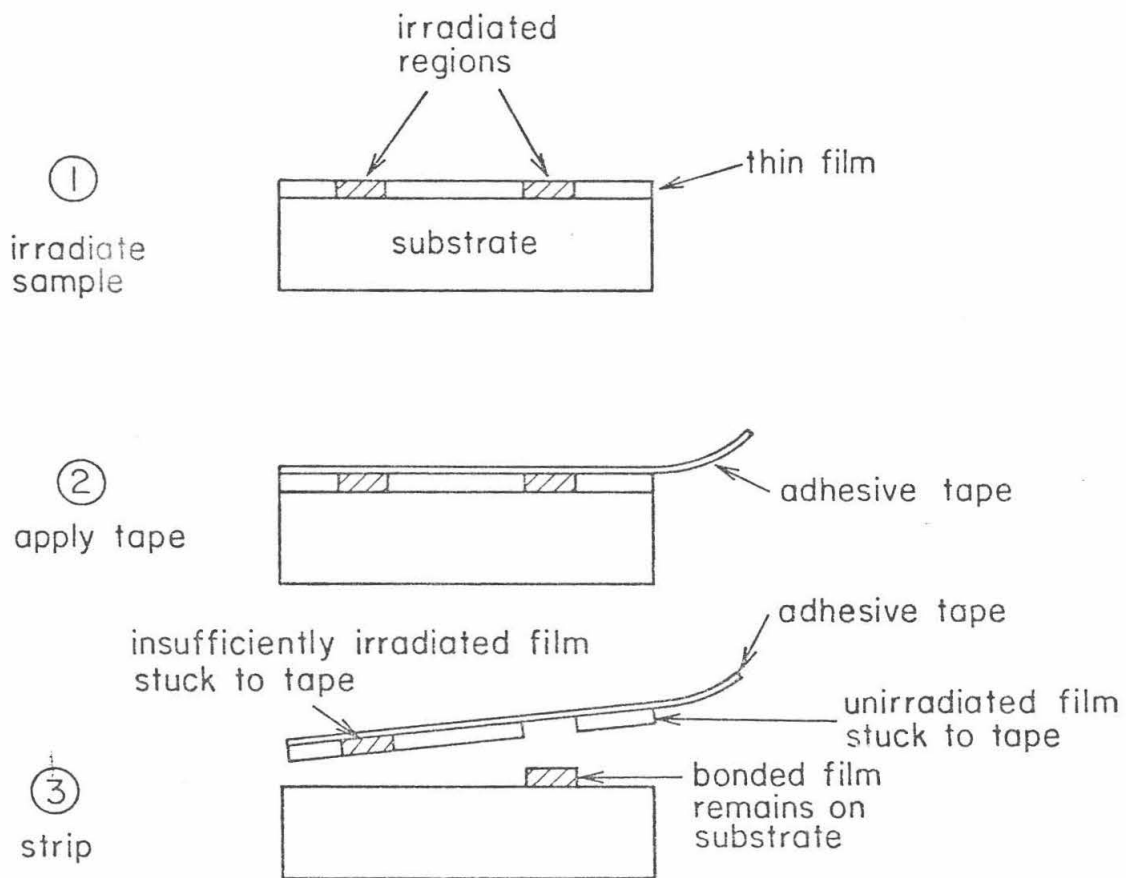


Figure 8
Schematic of the Loudspeaker Adhesion Tester
(see §3.2)

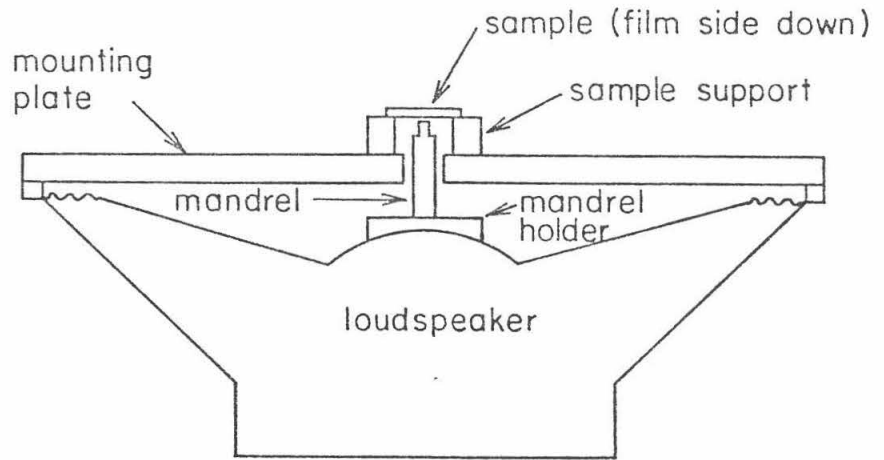
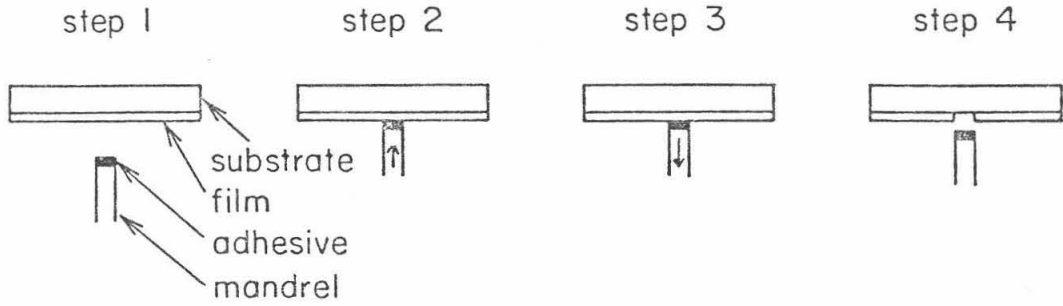


Figure 9
Operation Timing Sequence
for the
Loudspeaker Adhesion Tester
(see §3.2)

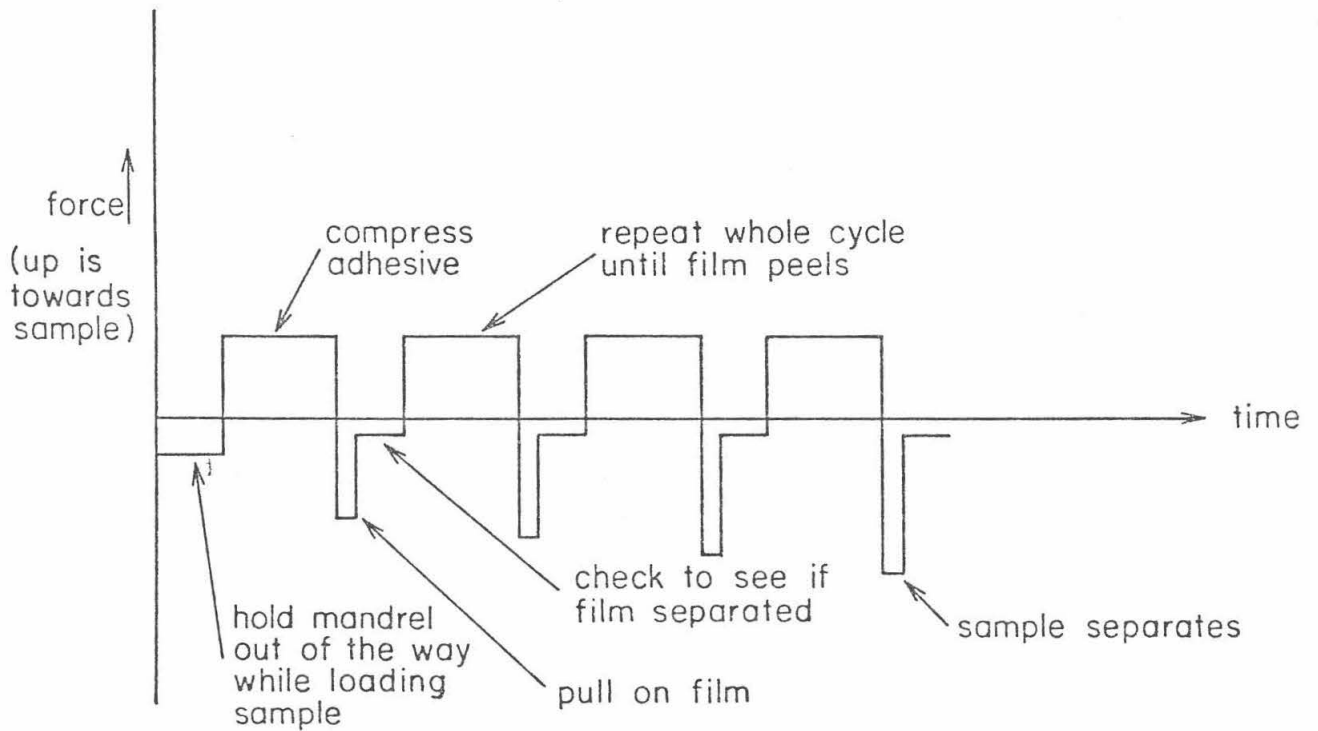


Figure 10
Electronics Block Diagram
for the
Loudspeaker Adhesion Tester
(see §3.2)

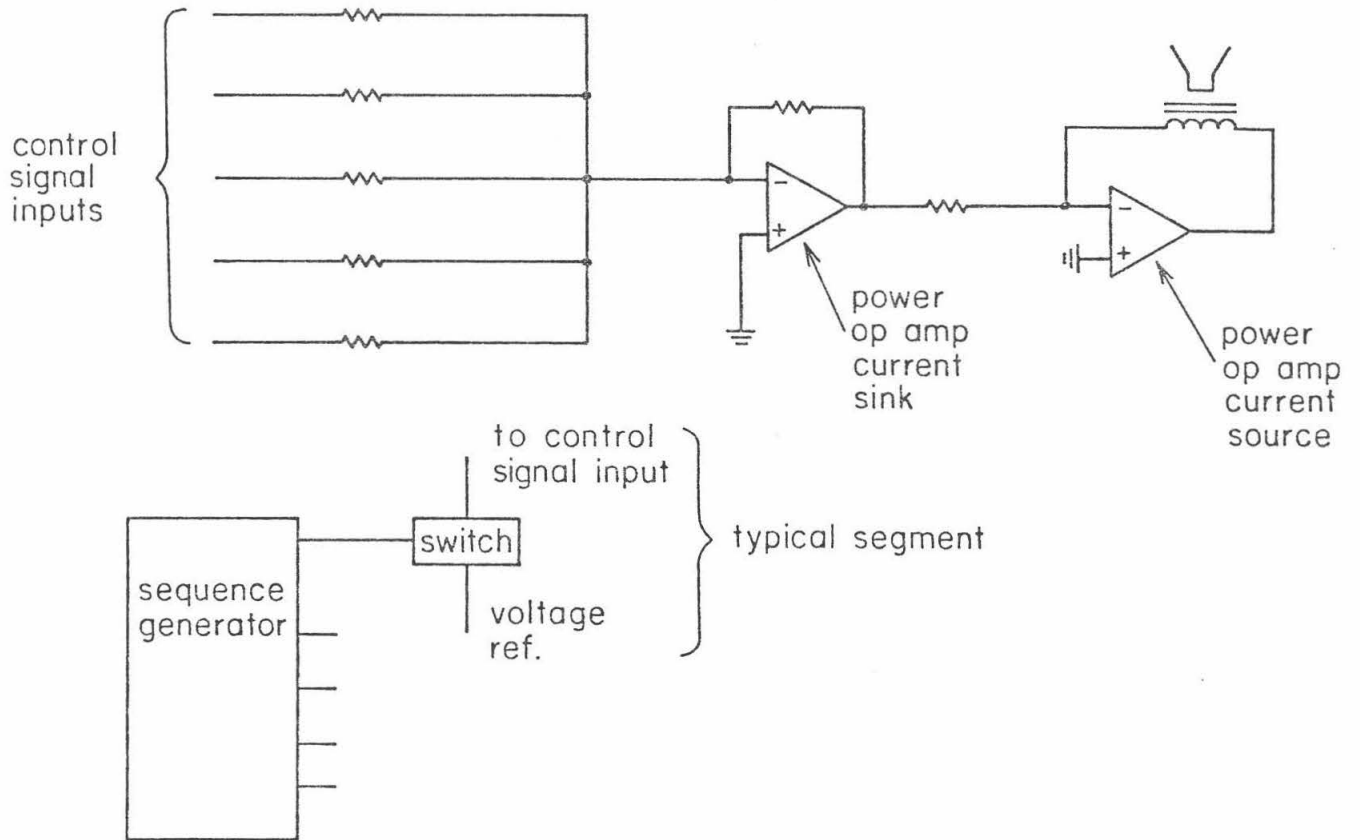


Figure 11
Target Setup
for
Rutherford Backscattering Experiments
(see §4.1)

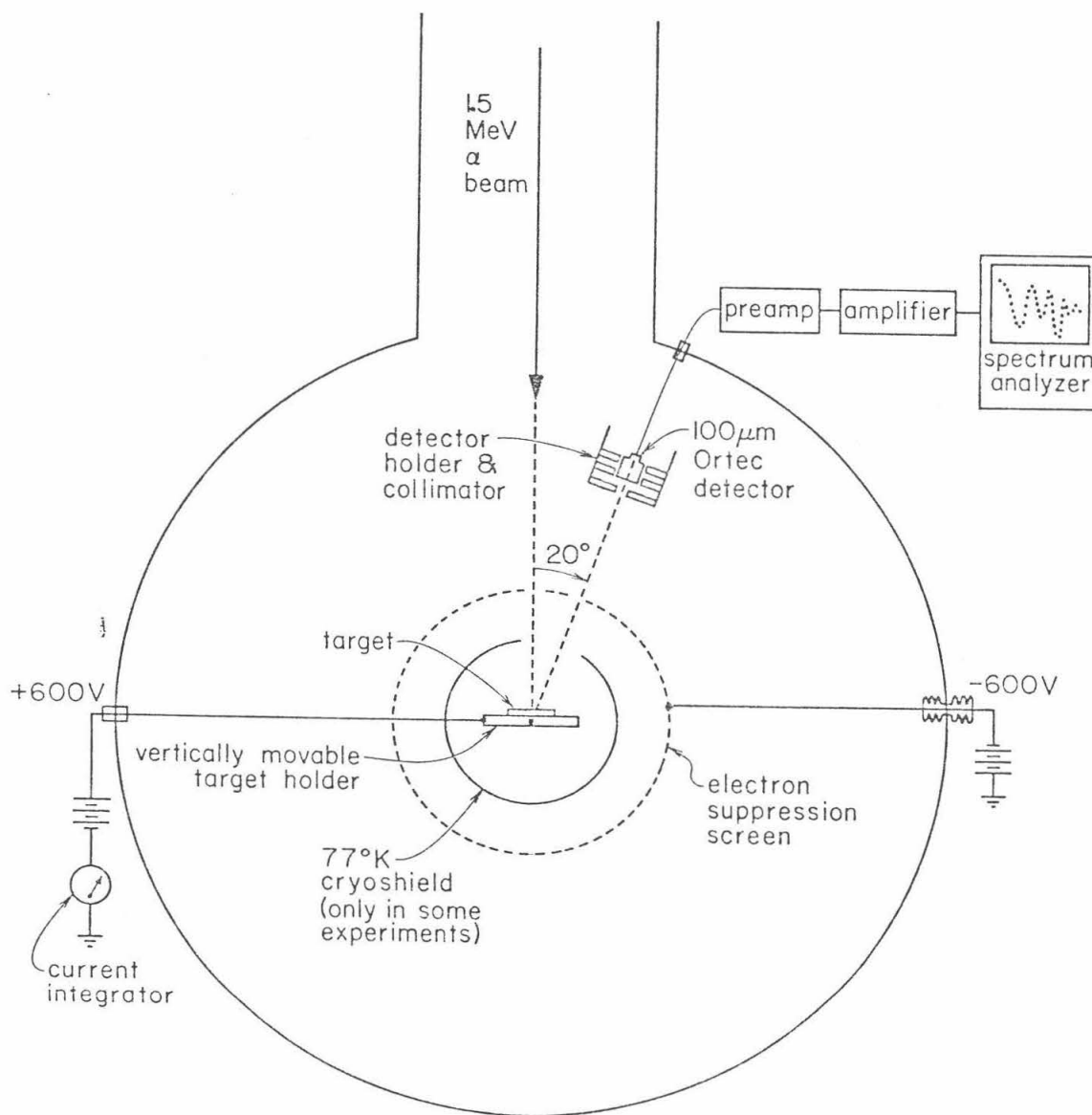


Figure 12
Backscattering Spectra
from
Gold on Fused Quartz Target
(see §4.1.1)

These spectra were taken from on and off of the beam spot of a piece of quartz which was irradiated with about $1 \times 10^{15} / \text{cm}^2$ of 20 MeV Cl. Compare to Fig. 22 which shows a schematic of a spectrum which indicates mixing.

Fig 12a is 9-Feb-82 Run 2 with bad channels edited out

Fig 12b is 9-Feb-82 Run 3

Fig. 12b Irradiated Au on Quartz

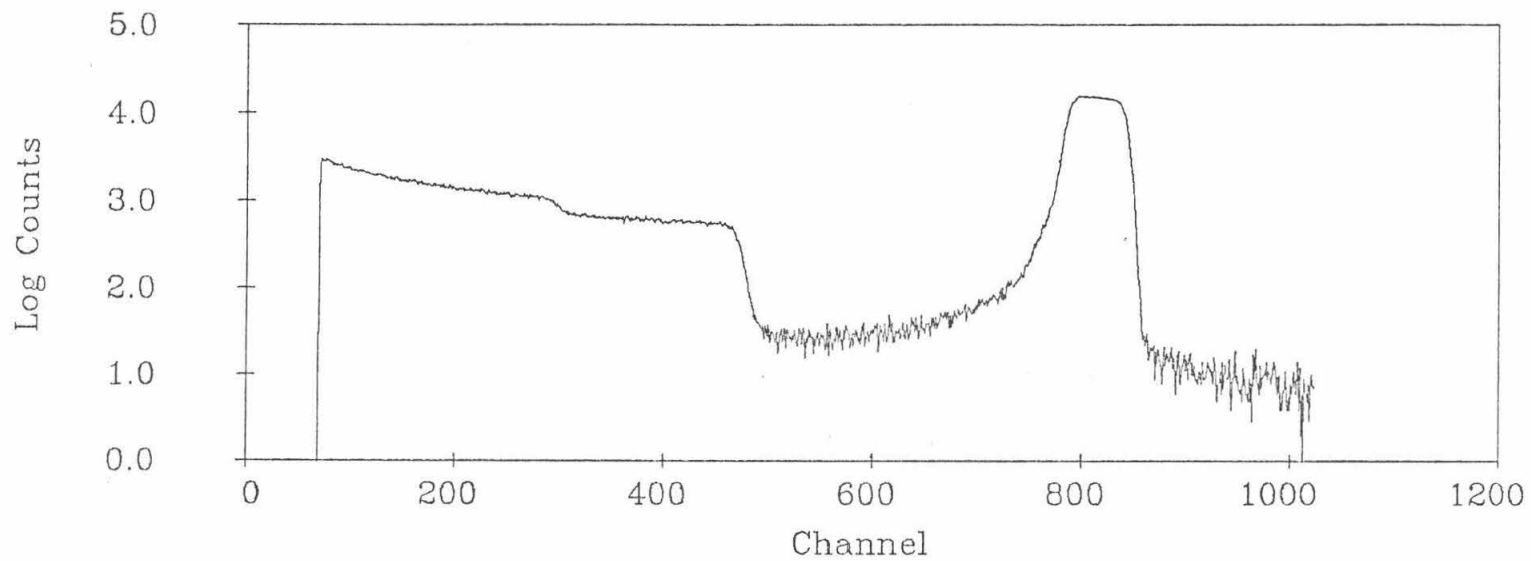


Fig. 12a Unirradiated Au on Quartz

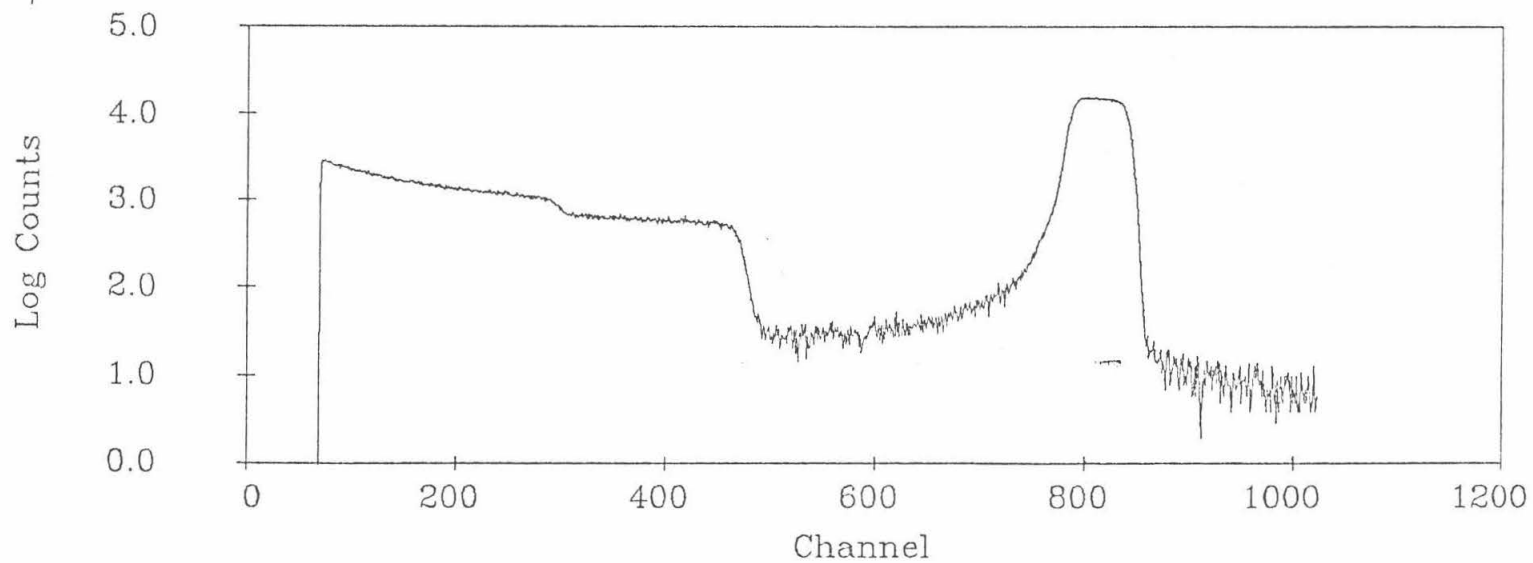


Figure 13
Backscattering Spectra
from
Stripped Gold on Fused Quartz Target
(see §4.1.1)

This RBS spectrum was taken from a sample that was irradiated with about $1 \times 10^{15} / \text{cm}^2$ of 20 MeV Cl and then stripped in aqua regia. To prevent electrical charging during the analysis, it was coated with $4 \mu\text{g} / \text{cm}^2$ Al. The peak labeled Ga is from residual gallium in the aluminum. The gold peak disappears when the sample is analyzed off of the Cl beam spot.

Fig 13 is 15-Feb-82 Run 1 with bad channels edited out

Fig. 13 Irradiated Au on Quartz with Au stripped

-48-

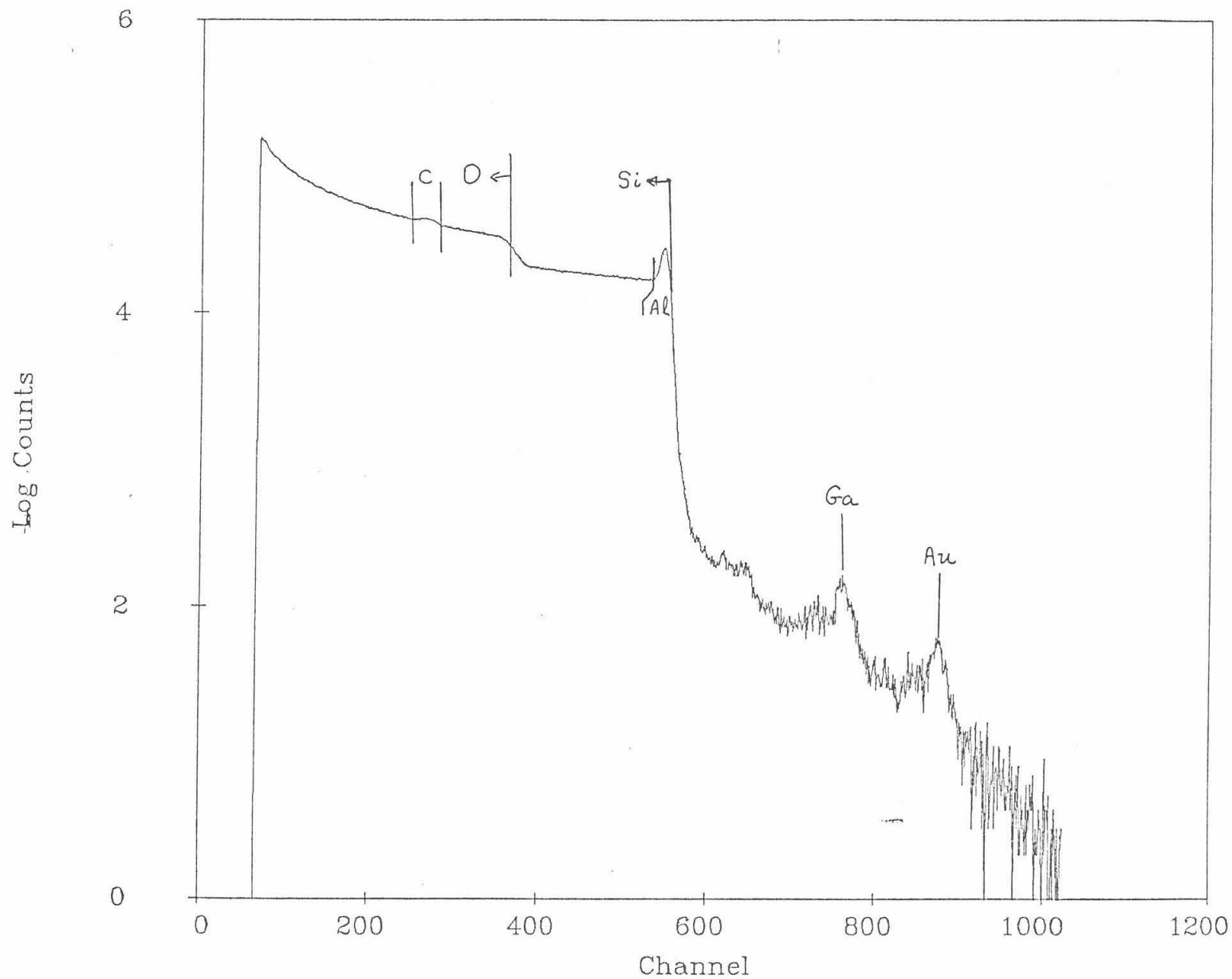


Figure 14
Backscattering Spectra
from
Stripped Gold on Ferrite Target
(see §4.1.1)

This spectrum is from the beam spot of a piece of Ni-Zn Ferrite which was irradiated with about $4 \times 10^{15} / \text{cm}^2$ of 20 MeV Cl. It was then etched in aqua regia and coated with $6 \mu\text{g} / \text{cm}^2$ Al.

Fig 13 is 19-Mar-82 Run 4

Fig. 14 irradiated Au on Ferrite with Au stripped

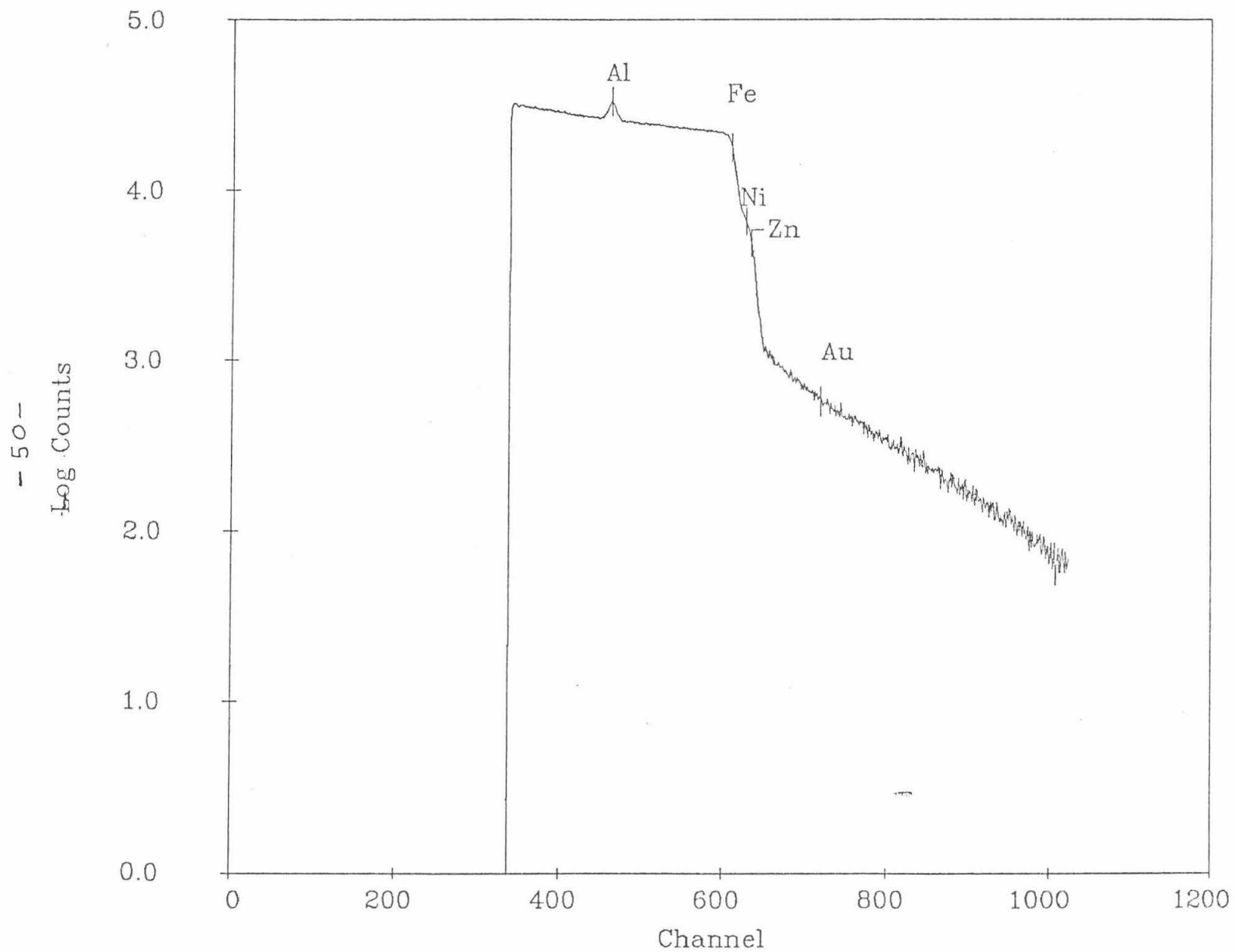


Figure 15
Schematic of Multilayer Ag/Si Target
(see §4.1.2)

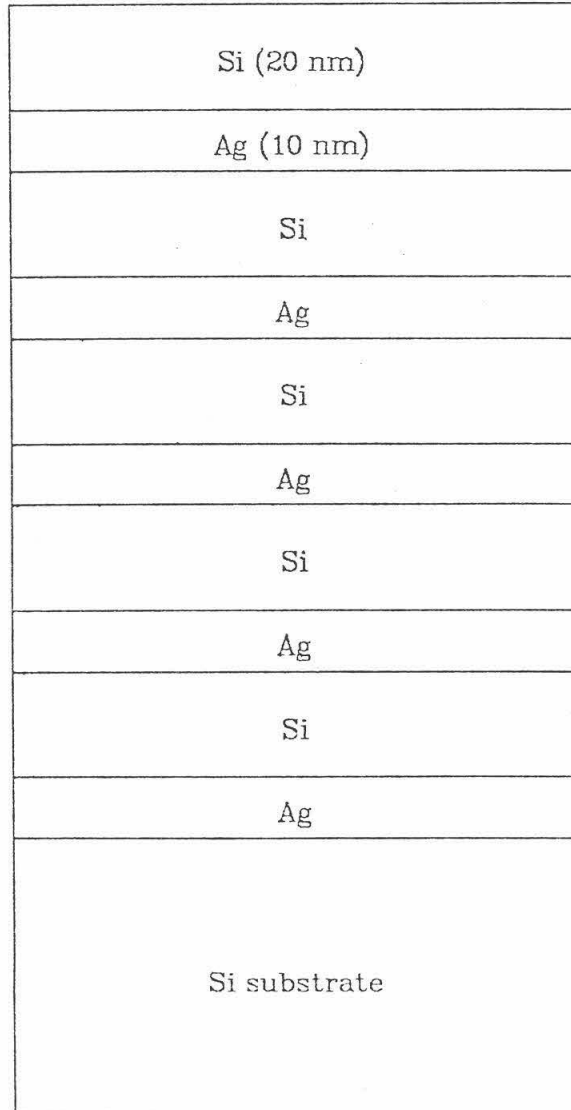


Figure 16
Resolution Calibration Spectrum
from
5 nm Au on SiO₂ Target
(see §4.1.2)

- a) This is the spectrum from a 5 nm Au on SiO₂ on Si target.
- b) This is an expansion of the Au peak of the previous spectrum. The energy scale is about 3 keV/channel so the width of this peak is about 22 keV FWHM.

Fig 16 is 3-Mar-1983 Run 10

Fig. 16b Expanded Au peak

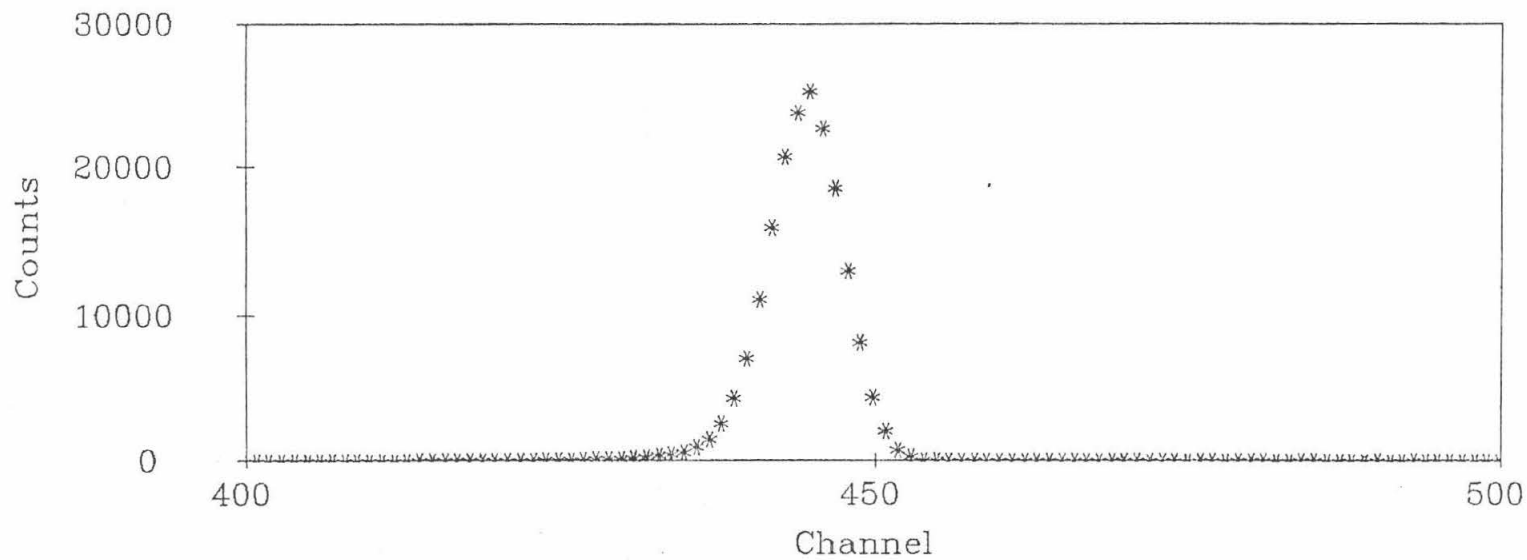


Fig. 16a Energy resolution calibration spectrum

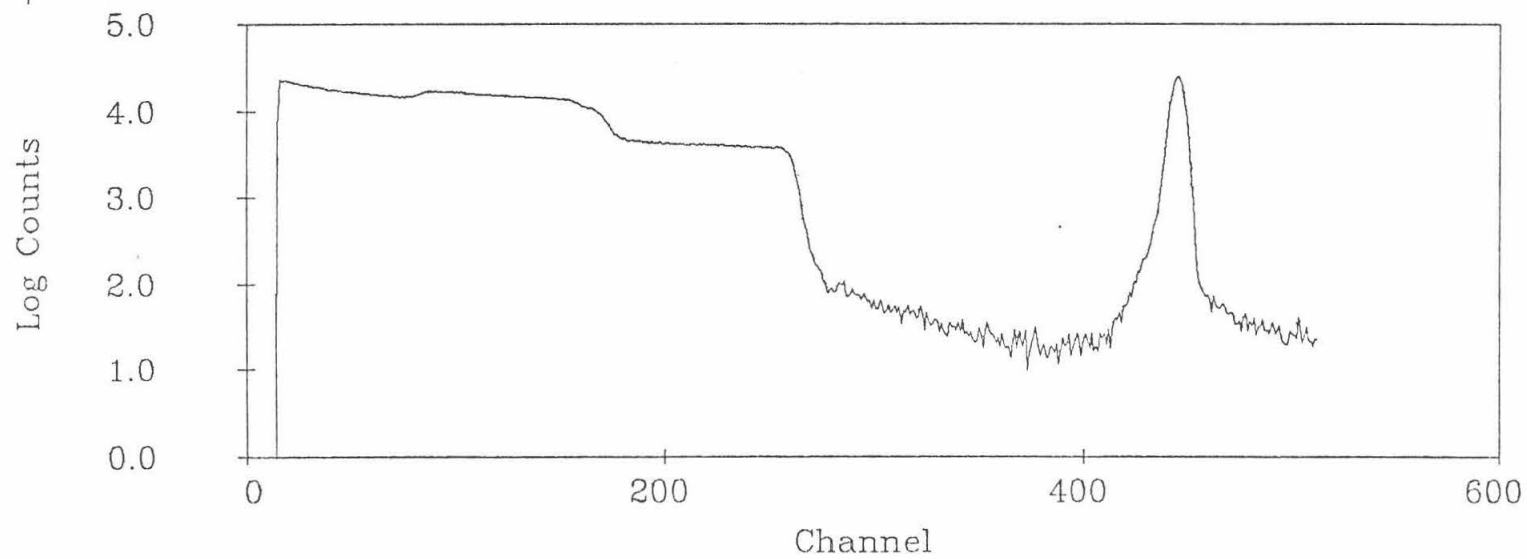


Figure 17
Backscattering Spectrum
from
Multilayer Ag/Si Target
(see §4.1.2)

This spectrum shows clearly the multilayer structure of the target used in this experiment. This type of target was used originally because it was expected that the mixing might be deep enough to sufficiently mix the layers that the contrast between layers would be substantially reduced in the spectrum (as is the case for low energy mixed Au on Si). However, even though that is not seen, the complexity of the spectrum allows one to get a good idea of the resolution of the system.

Fig 18 is 3-Mar-1983 Run 7

Fig. 17 Typical RBS Spectrum from Ag/Si stack target

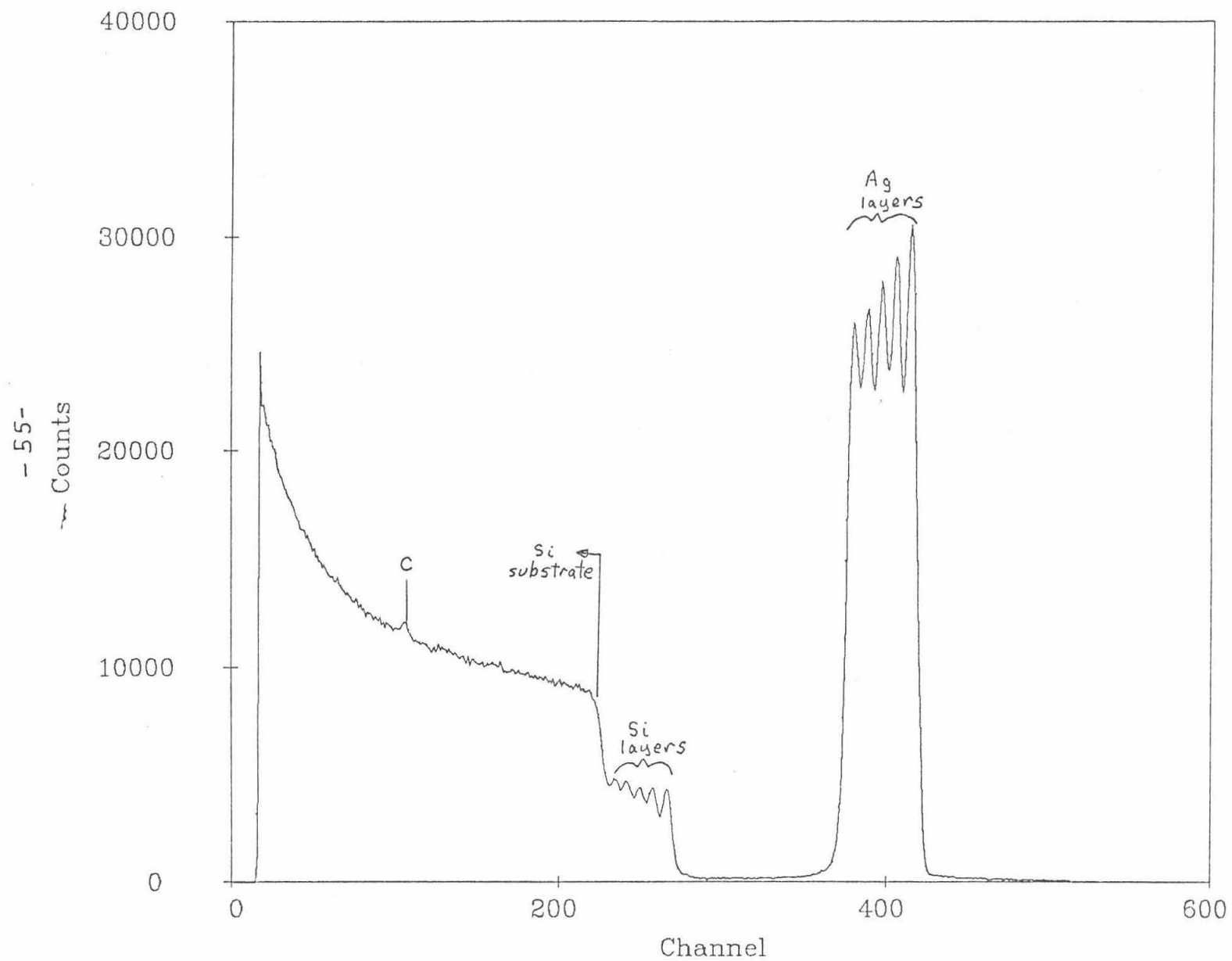


Figure 18
Expanded View of Ag Edge
on
Backscattering Spectrum
from
Multilayer Ag/Si Target
(see §4.1.2)

This spectrum is an expansion and comparison of the high edge of the silver peak from an irradiated and unirradiated part of the target. The curve plotted with the symbol + is from the irradiated area. The curve plotted with the symbol * is from the unirradiated area. The + curve is not raw data; it has been translated along the x-axis by 1.7 channels to the right and interpolated back to integral channel numbers to remove the effects of the slight carbon buildup on the target. Note how well the edges agree; there is no visible evidence for any broadening that might be caused by mixing.

The + curve is 3-Mar-1983 run 7, interpolated

The * curve is 3-Mar-1983 run 10

Fig. 18 Comparison of Ag edges on Ag/Si stack target

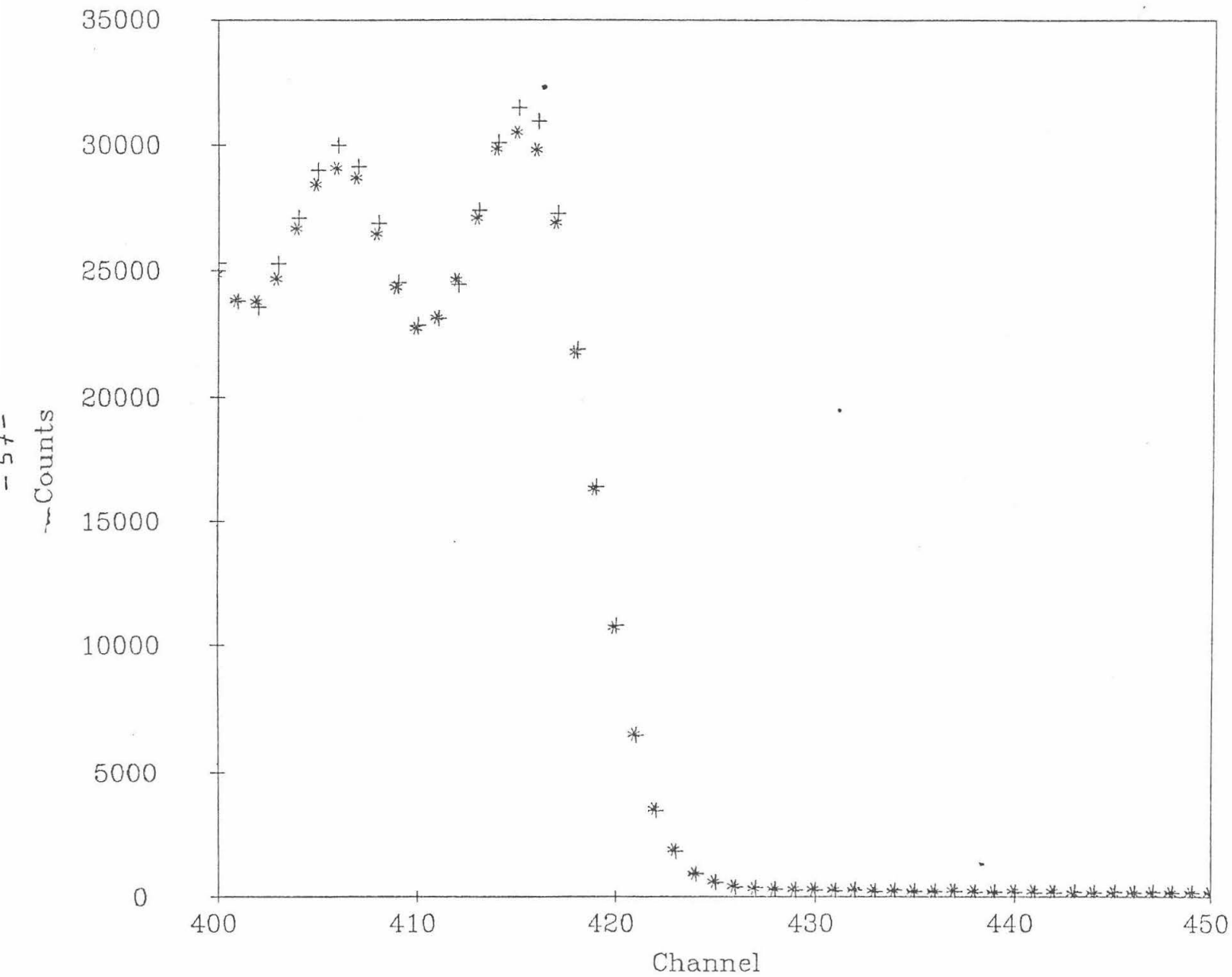


Figure 19

Schematic of Sample Preparation for TEM Study
(see §4.2)

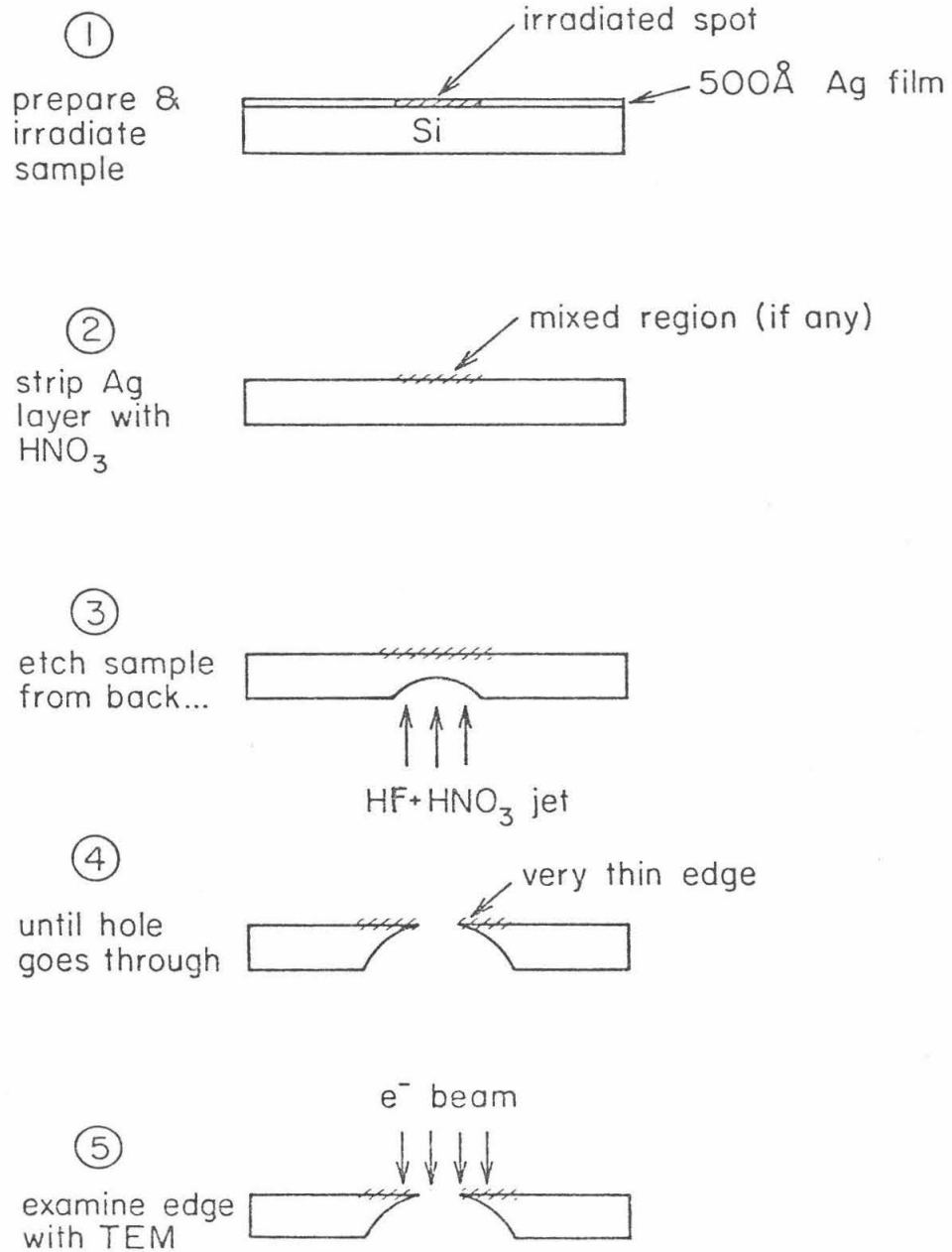


Figure 20
Picture of Typical Tape Test Sample
(see §4.3)

This is a sample of Au on Ta which was irradiated with 5 different beams to compare the adhesion caused by each beam. Spots within a horizontal row represent different fluences of the same beam particle. Different rows have been irradiated with different beams. The sharp threshold between spots which adhere and those which don't is quite clear. The total time required to do all the irradiations on a sample like this is about 4 hours. The actual size of the sample is about 1.5 inches in height.

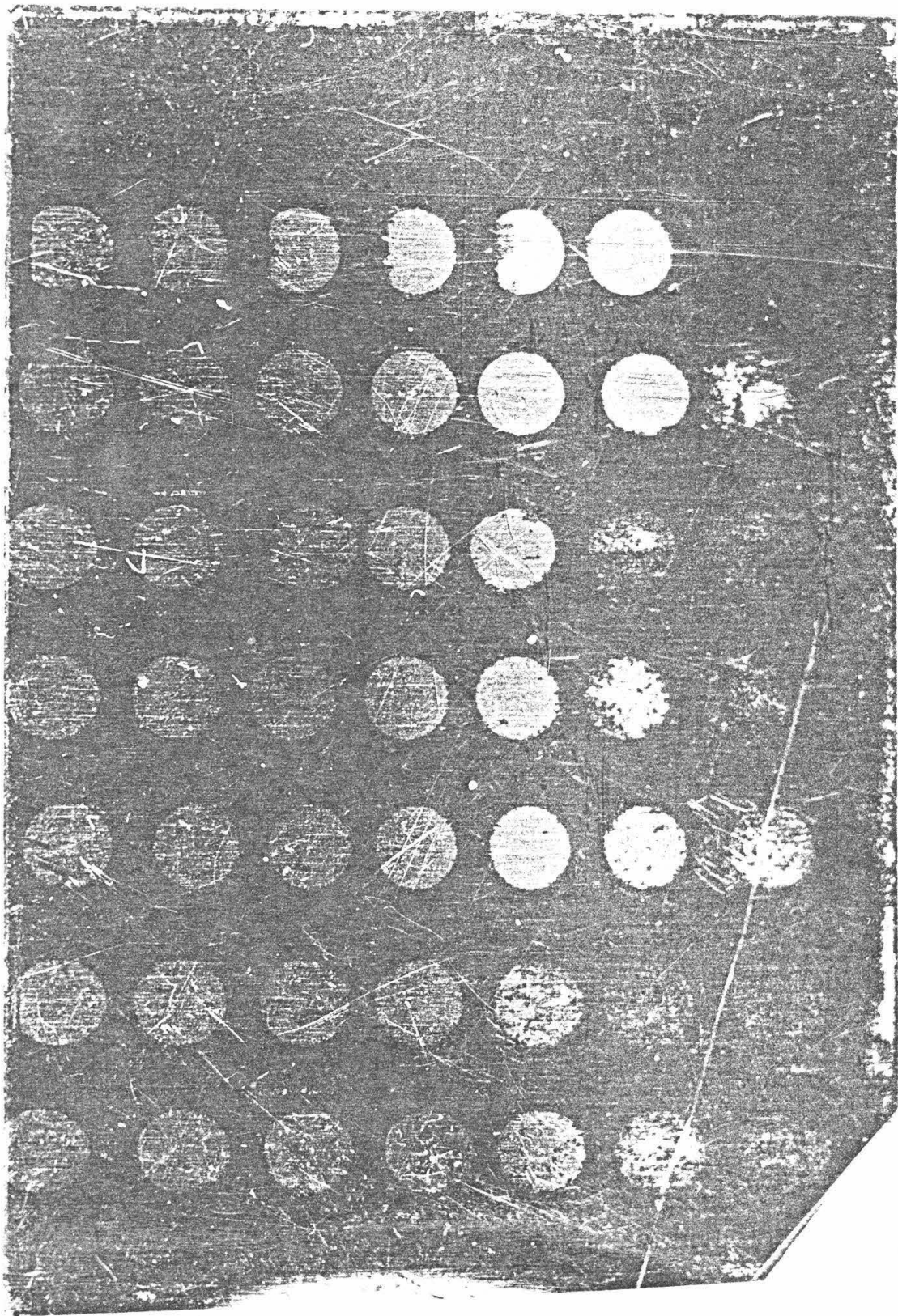


Figure 21
Plot of Beam Dose Required to Pass Tape Test
vs.
 dE/dx for the Ion Beam
on Au on Ta Targets
(see §4.3)

This plot shows the dependence of beam dose required to produce sufficient adhesion to pass the "Scotch Tape" test on the energy loss of the beam. The points plotted are

- 1 20 MeV Cl
- 2 7.2 MeV Cl
- 3 3.2 MeV Cl
- 4 12 MeV F
- 5 3.7 MeV F
- 6 1 MeV H
- 7 1 MeV He
- A 107 MeV Kr *
- B 35 MeV O *
- C 27 MeV Ar *
- D 87 MeV Ar *

and the line plotted is $Dose = 4.2 \times 10^{14} (dE/dx)^{-1.65}$. The point for protons has substantial uncertainties, since the peak adhesion for protons was very weak. However, the rest of the points should be reliable to within $\sqrt{2}$.

All points marked * above were run on the LBL 88" Cyclotron. As is described in §4.3, they have been adjusted downwards by a factor of 2 so that the 27 MeV Ar point lies on the curve from data obtained at Caltech. If the adjustment is omitted, the slope of the curve does not change significantly (since all the LBL points are internally consistent with this slope), but the multiplier for the doses increases by 15%.

Fig. 21 Beam Dose vs. dE/dx for Au on Ta

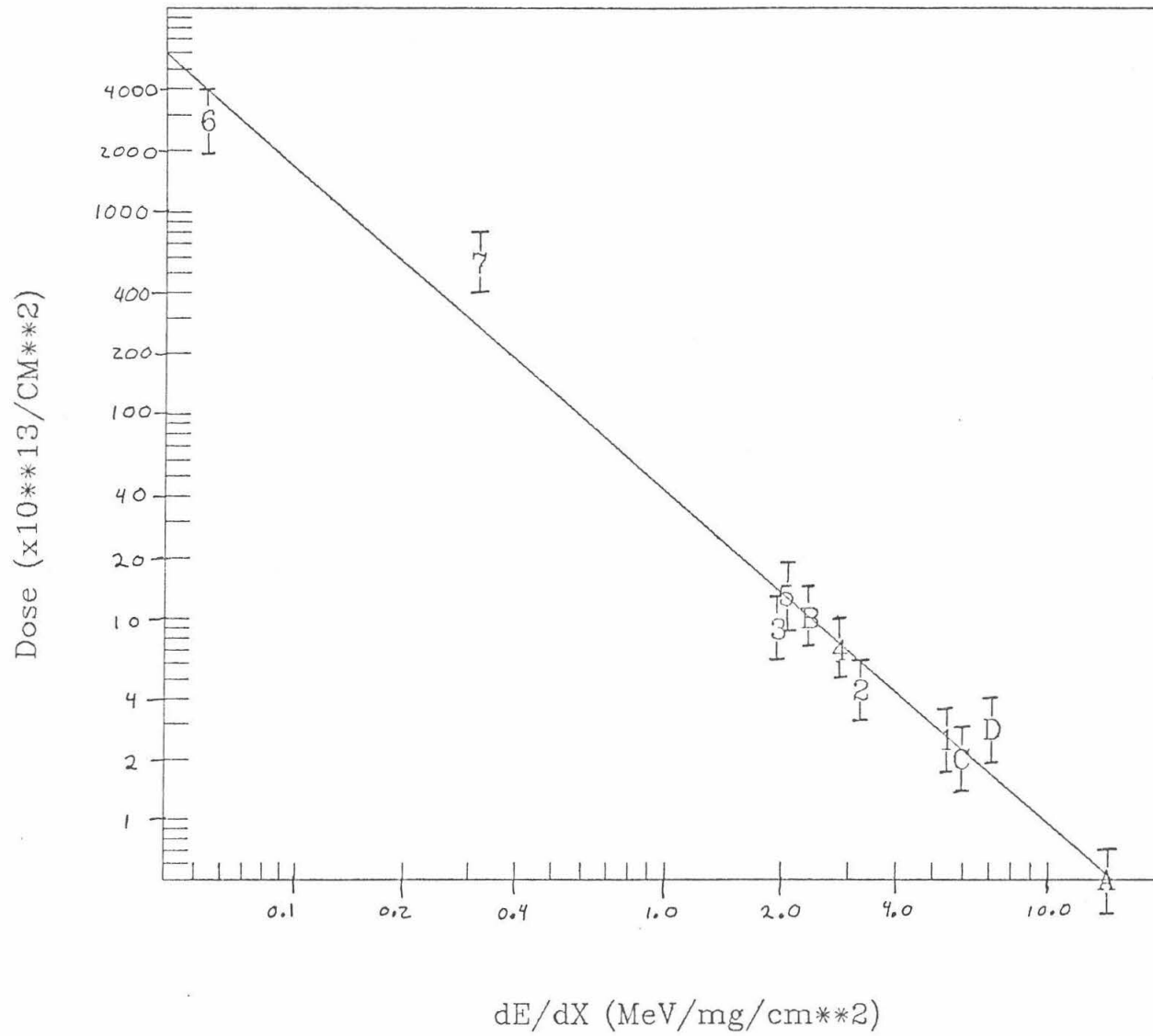
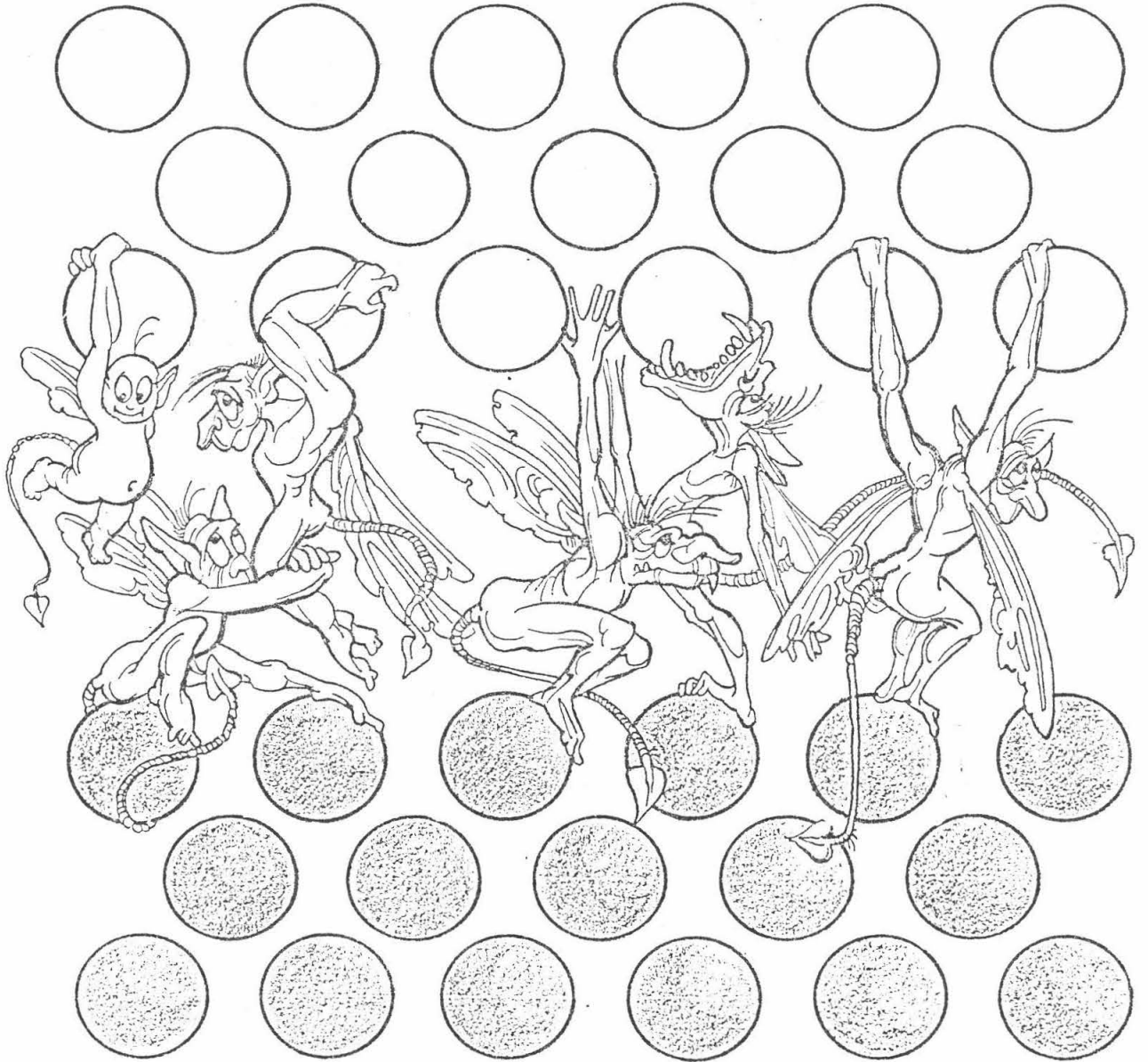


Figure 22
Most Interesting Mechanism Suggested
for
High Energy Heavy Ion Induced Adhesion
(See Acknowledgements)



BIBLIOGRAPHY

- (An77) H. H. Andersen and Zeigler, J. F., "Hydrogen, Stopping Power and Ranges in all Elements", *The Stopping and Ranges of Ions in Matter* 3, Pergamon Press, NY (1977)
- (Ch78) Chu, Mayer and Nicolet, *Backscattering Spectroscopy*, Academic Press, NY (1978)
- (Ch81) P. C. Chen, "Long Wavelength GaAsP/InP Semiconductor Lasers for Optical Communications", PhD. Thesis, Caltech (1981)
- (Fl75) R. L. Fleischer, *et. al.*, *Nuclear Tracks in Solids*, University of California Press, Berkeley, (1975)
- (Gr82) J. E. Griffith, *et. al.*, "Ion-Beam-Enhanced Adhesion in the Electronic Stopping Region", *Nuclear Instruments and Methods* 198 (1982), 607-609
- (Me82) C. K. Meins, *et. al.*, "Sputtering of UF₄ by High Energy Heavy Ions", Kellogg Radiation Laboratory, Caltech preprint BAP-34 (1982)
- (No70) L. C. Northcliffe and Schilling, R. F., "Range and Stopping Power Tables for Heavy Ions", *Nuclear Data Tables* 7, no. 3-4, Academic Press, NY, January 1970
- (Sa71) Saslow, *et. al.*, "Electronic Relaxation Times in Metals", *American Journal of Physics* 39, 1244 (1971)
- (Se82) L. E. Seiberling, *et. al.*, "The Sputtering of Insulating Materials by Fast Heavy Ions", *Nuclear Instruments and Methods* 198 (1982), 17-25
- (We82) B. Werner, *et. al.*, "Enhanced Adhesion from High Energy Ion Irradiation", Kellogg Radiation Laboratory, Caltech preprint BAP-36 (1982)
- (Wa82) C. Watson and Tombrello, T. A., "A Modified Lattice Potential Model of Enhanced Ion Erosion", Kellogg Radiation Laboratory, Caltech preprint BAP-33 (1982)

(Ze77)

J. F. Zeigler, "Helium, Stopping Power and Ranges in all Elements", *The Stopping and Ranges of Ions in Matter* 4, Pergamon Press, NY (1977)

